Since January 2020 Elsevier has created a COVID-19 resource centre with free information in English and Mandarin on the novel coronavirus COVID-19. The COVID-19 resource centre is hosted on Elsevier Connect, the company's public news and information website.

Virology 409 (2011) 175–188

Contents lists available at ScienceDirect

Virology

journal homepage: www.elsevier.com/locate/yviro

Antiviral activities of ISG20 in positive-strand RNA virus infections

Zhi Zhou [a,g], Nan Wang [b], Sara E. Woodson [c], Qingming Dong [b], Jie Wang [b], Yuqiong Liang [a], Rene Rijnbrand [a,1], Lai Wei [d], Joan E. Nichols [e], Ju-Tao Guo [f], Michael R. Holbrook [c,2], Stanley M. Lemon [a,e,3], Kui Li [b,*]

[a] Department of Microbiology and Immunology, Institute for Human Infections and Immunity, University of Texas Medical Branch, Galveston, TX, USA
[b] Department of Molecular Sciences, University of Tennessee Health Science Center, Memphis, TN, USA
[c] Department of Pathology, Institute for Human Infections and Immunity, University of Texas Medical Branch, Galveston, TX, USA
[d] Peking University Hepatology Institute, Peking University People's Hospital, Beijing, China
[e] Department of Internal Medicine, Institute for Human Infections and Immunity, University of Texas Medical Branch, Galveston, TX, USA
[f] Department of Microbiology and Immunology, Drexel University College of Medicine, Doylestown, PA, USA
[g] Department of Infectious Diseases, the Second Teaching Hospital, Chongqing Medical University, Chongqing, China

ARTICLE INFO

Article history:
Received 19 July 2010
Returned to author for revision 5 August 2010
Accepted 6 October 2010
Available online 30 October 2010

Keywords:
ISG20
Interferon
Hepatitis C virus
Bovine viral diarrhea virus
Yellow fever virus
Hepatitis A virus
Severe acute respiratory syndrome coronavirus
ISG20L1
ISG20L2
Antiviral
Innate immunity

ABSTRACT

ISG20 is an interferon-inducible 3′–5′ exonuclease that inhibits replication of several human and animal RNA viruses. However, the specificities of ISG20's antiviral action remain poorly defined. Here we determine the impact of ectopic expression of ISG20 on replication of several positive-strand RNA viruses from distinct viral families. ISG20 inhibited infections by cell culture-derived hepatitis C virus (HCV) and a pestivirus, bovine viral diarrhea virus and a picornavirus, hepatitis A virus. Moreover, ISG20 demonstrated cell-type specific antiviral activity against yellow fever virus, a classical flavivirus. Overexpression of ISG20, however, did not inhibit propagation of severe acute respiratory syndrome coronavirus, a highly-pathogenic human coronavirus in Huh7.5 cells. The antiviral effects of ISG20 were all dependent on its exonuclease activity. The closely related cellular exonucleases, ISG20L1 and ISG20L2, did not inhibit HCV replication. Together, these data may help better understand the antiviral specificity and action of ISG20.

Introduction

Eukaryotes have evolved numerous intrinsic mechanisms to combat microbial infections. The interferon (IFN) system is a major innate antiviral pathway that is present in vertebrate cells. It is rapidly activated in a tightly regulated fashion in response to viral infections. Viral nucleic acids in viral genomes or generated during viral replication present major pathogen associated molecular patterns (PAMPs) to various cellular PAMP receptors, including the membrane bound toll-like receptors (TLRs) or the cytoplasmic RIG-like receptors (RLRs). Upon engagement with their cognate ligands, the TLRs and RLRs recruit distinct adaptor proteins and transmit signals to downstream kinases, culminating in the activation of the latent transcription factors, IRF3 and NF-kB, which coordinately regulate synthesis of type I IFNs (IFN-β and -α) (Yoneyama and Fujita, 2010). Once secreted, IFNs act in a paracine/autocrine fashion through cell surface IFN receptors, leading to the induction of hundreds of IFN stimulated genes (ISGs) via the Jak-STAT pathway (Sen, 2001; Stark et al., 1998). Although considerable progress has been made in understanding the biological functions of a number of ISGs, much remains to be learned about the role of the majority of ISGs in innate antiviral defense. Apart from inducing cellular genes with direct antiviral effects, IFNs also regulate activation of professional immune cells, shaping subsequent adaptive immunity to virus infections (Sen, 2001; Stark et al., 1998; Yoneyama and Fujita, 2010).

* Corresponding author. 401B Molecular Sciences Building, University of Tennessee Health Science Center, 858 Madison Avenue, Memphis, TN 38163, USA. Fax: +1 901 448 7360.
E-mail address: kli1@uthsc.edu (K. Li).
[1] Current address: Vertex Pharmaceuticals, Cambridge, MA 02139, USA.
[2] Current address: NIAID-Integrated Research Facility, 8200 Research Plaza, Fort Detrick, Frederick, MD 21702, USA.
[3] Current address: Department of Medicine, Center for Translational Immunology, and the Lineberger Comprehensive Cancer Center, The University of North Carolina at Chapel Hill, Chapel Hill, NC 27599-7295, USA.

0042-6822/$ – see front matter © 2010 Elsevier Inc. All rights reserved.
doi:10.1016/j.virol.2010.10.008

In addition to serving as PAMPs for activation of the IFN system, viral nucleic acids represent excellent targets which are subject to the direct action of cellular antiviral proteins. Among the latter the RNase L pathway represents a principal component of IFN's antiviral effector mechanisms. A latent, ubiquitous endonuclease, RNase L is activated by short oligoadenylates produced by the IFN-inducible, 2′5′-oligoadenylate synthetases following viral infection. Activated RNase L exerts direct antiviral effect by cleaving and degrading viral RNAs. It also cleaves cellular 18S and 28S rRNAs, resulting in inhibition of protein synthesis and cellular apoptosis, thereby preventing viral propagation (Silverman, 2007). RNase L-deficient mice have enhanced susceptibility to infections by encephalomyocarditis virus (EMCV), Coxsackievirus, herpes simplex virus 1 and West Nile virus (Flodstrom-Tullberg et al., 2005; Samuel et al., 2006; Zheng et al., 2001; Zhou et al., 1997). Nevertheless, analyses of mice triply deficient for the three well-characterized antiviral pathways, PKR, RNase L, and Mx demonstrated the presence of alternative effector mechanisms which mediate IFN's antiviral actions (Zhou et al., 1999).

The IFN-stimulated gene 20 kDa protein (ISG20) has recently emerged as a second IFN-regulated RNase that inhibits RNA virus replication (Degols et al., 2007). ISG20, along with the closely related ISG20L1 (a.k.a., apoptosis-enhancing nuclease, AEN) and ISG20L2, belongs to the yeast RNA exonuclease 4 homolog (REX4) subfamily within the DEDDh exonuclease family (Coute et al., 2008). Proteins of this family can have both RNase and DNase activities; all have a large structurally related, 150-aa long exonuclease domain (ExoIII) that contains three distinct exonuclease motifs termed Exo I, Exo II and Exo III defined by four conserved acidic amino acids, DEDD and a conserved histidine residue (Degols et al., 2007). Biochemical analyses demonstrated that ISG20 is a 3′–5′ exonuclease that has a preference for single-stranded (ss) RNA over ssDNA (Nguyen et al., 2001). When overexpressed in vitro, ISG20 restricted infections by EMCV, vesicular stomatitis virus, influenza virus, HIV and Sindbis virus, although the antiviral efficiencies varied (Espert et al., 2003, 2005; Zhang et al., 2007). ISG20 also inhibited the replication of subgenomic, genotype 1b hepatitis C virus (HCV) RNA replicons in HEK293 cells (Jiang et al., 2008).

The mechanism underlying the antiviral action of ISG20 remains poorly understood, as does its viral specificity (Degols et al., 2007). The former is believed to involve degradation of viral RNAs by means of the 3′–5′ exonuclease activity of ISG20, although possible actions on cellular factors cannot be excluded (Degols et al., 2007). The antiviral action of ISG20 is thought to operate poorly on double stranded regions, as the RNase activity of ISG20 is negatively regulated by the presence of a stem-loop structure at the 3′end of the RNA substrate (Nguyen et al., 2001). However, only a small number of RNA viruses have been tested thus far, precluding a better understanding of the specificity and mechanism of action of ISG20. Furthermore, it is not known whether the antiviral effect is shared by other exonucleases that are closely related to ISG20. In this study, we have compared in cell culture the effects of ISG20 on replication of several positive-strand RNA viruses from distinct viral families, including *Flaviviridae* [HCV, bovine viral diarrhea virus (BVDV) and yellow fever virus (YFV)], *Piconaviridae* [hepatitis A virus (HAV)] and *Coronaviridae* [severe acute respiratory syndrome coronavirus (SARS-CoV)]. We show that (1) ISG20 inhibits replication of genotype 2a subgenomic HCV RNAs and cell culture derived HCV, and that of HAV in cultured hepatoma cells; (2) ISG20 restricts BVDV propagation in bovine kidney cells; (3) ISG20 demonstrates cell-type specific antiviral effect against YFV, a classical flavivirus; (4) ISG20 does not inhibit SARS-CoV, a highly pathogenic novel human coronavirus in Huh7.5 cells; 5) the antiviral effect against HCV by ISG20 is not shared with ISG20L1 and ISG20L2. Our data characterize the antiviral activities of ISG20 against distinct positive strand RNA viruses and may help to better understand the specificity and action of ISG20 in IFN-mediated antiviral innate immunity.

Results

Characterization of Huh7.5 cells stably expressing human ISG20 and a related, catalytically inactive mutant ISG20

To determine how ISG20 affects HCV replication in hepatocytes, we developed Huh7.5 cells that stably express human ISG20 (designated as 7.5-ISG20) and as controls, cells expressing the catalytically inactive, D94G mutant ISG20 that is deficient in exonucleasae activity (Nguyen et al., 2001) (designated as 7.5-ISG20m) and those expressing the empty vector (designated as 7.5-Bsr), respectively, using retroviral-mediated gene transfer. Huh7.5 cells represent an Huh7 subline that is highly permissive for HCV replication (Blight et al., 2002). In addition, Huh7 derived cells are susceptible to many RNA viruses of distinct viral families (Devaraj et al., 2007; Guix et al., 2007; Hattermann et al., 2005; Keskinen et al., 1999; Lohmann et al., 1999; Muller et al., 2007; Tang et al., 2005; Yi and Lemon, 2002). By establishing Huh7.5 cells stably expressing ISG20/ISG20m, we were able to evaluate the effect of this ISG on replication of many different viruses. To eliminate phenotypic differences derived from variations among individual cell clones, we utilized stable cell pools instead of clonal cell lines. The ectopically expressed ISG20 (Fig. 1A) and ISG20m (data not shown) were distributed in both nucleus and cytoplasm, and could be readily detected in 7.5-ISG20 and 7.5-ISG20m cells by immunoblot analysis using antibodies directed either against the myc epi-tag that was introduced at the C-terminus of ISG20 (Fig. 1B, upper panel) or against the ISG20 protein itself (lower panel), but not in the control vector expressing 7.5-Bsr cells. Although they were stably expressed at high levels (Fig. 1C), ISG20 and ISG20m did not alter growth characteristics of Huh7.5 cells (Fig. 1D, compare 7.5-ISG20 and 7.5-ISG20m vs 7.5-Bsr cells), nor did they affect the RIG-I signaling defect in Huh7.5 cells (Sumpter et al., 2005) as determined by the absence of ISG56 induction following Sendai virus infection, irrespective of ISG20/ISG20m expression status (Fig. 1E, compare lanes 3, 5, and 7 vs 9).

ISG20 inhibits replication of genotype 2a subgenomic HCV RNA replicons and JFH1 virus infection by means of its catalytic activity in hepatoma cells

Ectopic expression of ISG20 in HEK293 cells inhibits the replication of a bicistronic, selectable subgenomic HCV-N (genotype 1b) RNA replicon (Jiang et al., 2008). To determine how ISG20 affects HCV replication in hepatocytes, we first compared 7.5-ISG20, 7.5-ISG20m and 7.5-Bsr cells for supporting the replication of genotype 2a JFH1 RNAs. We constructed a monocistronic subgenomic JFH1 RNA replicon, SGRm-JFH1BlaRL, in which the coding sequences for most of the HCV structural proteins (core-E1-E2-p7) and NS2 were replaced by cDNA sequences encoding the blasticidin resistance gene product directly fused to the N-terminus of Renilla luciferase, FMDV autoprotease and ubiquitin, with the latter two directing processing at the N-terminus of NS3 (Fig. 2A). SGRm-JFH1BlaRL RNA, but not the RNA-dependent RNA polymerase defective GND mutant, replicated continuously and robustly in transfected Huh7.5 cells, expressing renilla luciferase as a measure of viral RNA amplification (Data not shown). SGRm-JFH1BlaRL replicated efficiently with similar kinetics in 7.5-Bsr and 7.5-ISG20m cells, reaching a plateau at 48 to 96 h posttransfection (Fig. 2A). In contrast, its replication was severely impaired in 7.5-ISG20 cells. At all time points examined, the replication levels of SGRm-JFH1BlaRL RNA were always 5- to 10-fold lower than those in 7.5-Bsr and 7.5-ISG20m cells (Fig. 2A). As controls, the GND mutant replicon failed to replicate in any of these three Huh7.5-derived cells (Fig. 3B).

We next determined how expression of ISG20 and ISG20m affects propagation of JFH1 virus. In agreement with data from the replicon experiments, we found that infectious progeny JFH1 virus release in

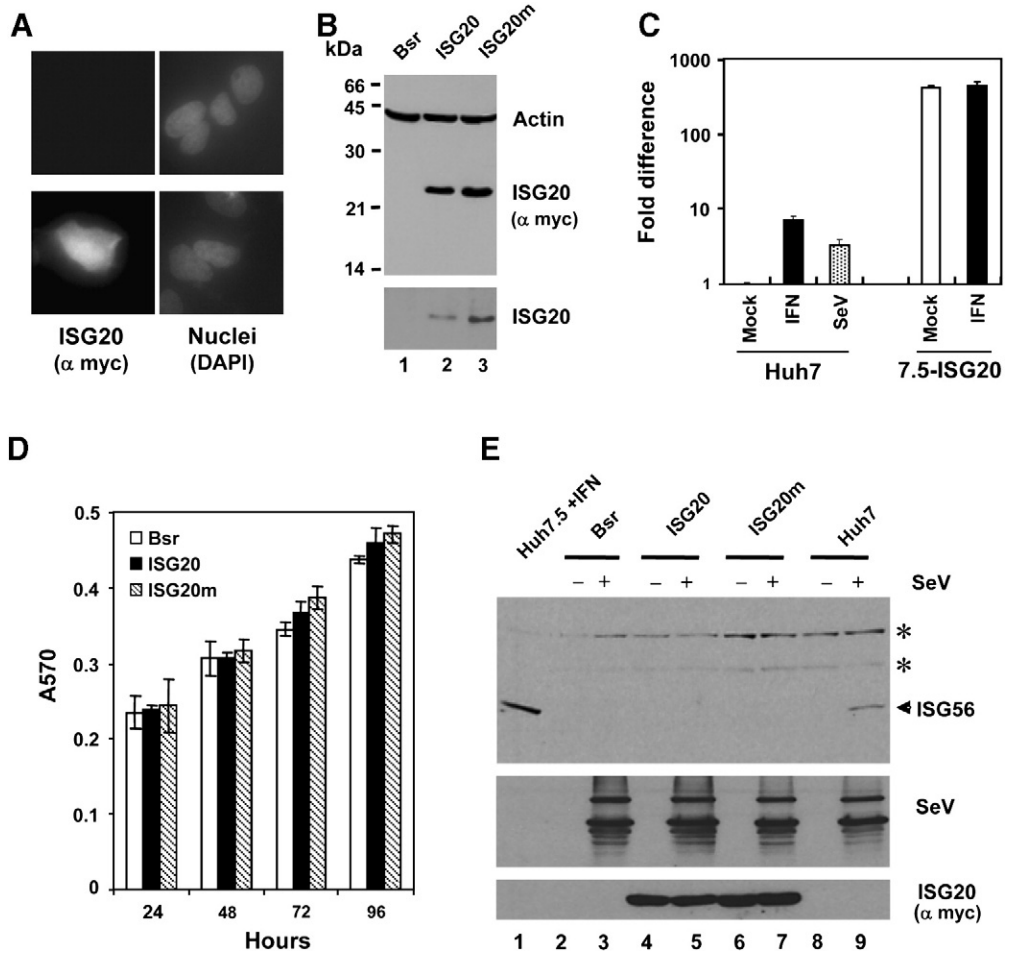

Fig. 1. Characterization of Huh7.5 cells stably expressing human ISG20 or its catalytically inactive mutant (ISG20m). (A) Immunofluorescence staining of ISG20 expression (using anti-myc mAb) in Huh7.5 cells mock-transfected (upper panels) or transiently transfected with a vector encoding myc-tagged ISG20 (lower panels). DAPI staining of nuclei was shown in the right panels. Similar subcellular localization of ISG20 was observed in Huh7.5 cells stably transduced with human ISG20 (7.5-ISG20) or the D94G mutant ISG20 (7.5-ISG20m) (data not shown). (B) Immunoblot analysis of ISG20 expression in 7.5-ISG20, 7.5-ISG20m and cells stably expressing the empty vector (Bsr). ISG20/ISG20m was probed with anti-myc mAb (upper panel) and ISG20 (lower panel), respectively. Actin was detected with mAb anti-actin (upper panel), to demonstrate equal sample loading. Note that ISG20m expressed to a slightly higher level than ISG20. It is unknown whether this reflects an auto-regulation of its own expression by ISG20. (C) Realtime PCR analysis of ISG20 mRNA levels in Huh7 and 7.5-ISG20 cells mock-treated or stimulated with IFN-α (500 U/ml) or infected with SeV (100 HAU/ml) for 16 h. mRNA abundances were normalized to cellular 28S rRNA. Fold differences were calculated by dividing normalized mRNA abundance following various treatments by that of the mock-treated Huh7 cells. IFN-α induced endogenous ISG20 expression by 7- to 15-fold in Huh7 and 7.5-ISG20 cells, while SeV upregulated ISG20 mRNA by 3-fold in Huh7 cells. (D) Triplicate wells of cells in 24-well plates were cultured for the indicated time periods and cell proliferation assessed by MTT assay. (E) ISG20 or ISG20m expression does not reconstitute the RIG-I signaling defect in Huh7.5 cells. 7.5-Bsr, 7.5-ISG20, 7.5-ISG20m, and normal Huh7 cells were mock infected or infected with 100 HAU/mL of SeV for 16 h prior to cell lysis and immunoblot analysis of ISG56, SeV and ISG20 (using anti-myc tag mAb). Asterisks in ISG56 panel denote nonspecific bands. Huh7.5 cells treated with recombinant human IFN-α for 16 h (lane 1) was included as a positive control for ISG56 expression.

culture supernatants was reproducibly 7- to 10-fold lower in 7.5-ISG20 cells than that in 7.5-Bsr and 7.5-ISG20m cells at 48–72 h postinfection (MOI = 0.05), while JFH1 virus yields were similar between the latter two cultures (Fig. 2B). In aggregate, ISG20 not only inhibits replication of genotype 1b HCV RNA replicons in HEK293 cells (Jiang et al., 2008), but also acts to restrict genotype 2a HCV RNA replication and JFH1 virus propagation in cultured hepatocytes. The exonuclease activity is required for the antiviral activity of ISG20 against HCV.

ISG20 does not accelerate the degradation of HCV RNAs, nor does it inhibit HCV IRES-dependent translation

The antiviral action of ISG20 is thought to involve the degradation of viral RNAs by the 3′–5′ exonuclease activity of ISG20 (Degols et al., 2007). To determine whether ISG20 promotes HCV RNA degradation, we determined the stability of modified subgenomic HCV RNAs encoding a luciferase reporter gene and also containing a lethal mutation in the NS5B RNA-dependent RNA polymerase (Fig. 3A). Upon introduction into cells, these HCV RNAs express Renilla (SGRm-JFH1BlaRL/GND) or firefly (NmLuc/ΔGDD) luciferases directed by HCV IRES (SGRm-JFH1BlaRL/GND) or EMCV IRES (NmLuc/ΔGDD), respectively. The luciferase activity serves as a read-out for HCV RNA abundance. Due to the inability of these HCV RNAs to replicate, the decay rate in luciferase activity represents the rate of HCV RNA degradation. After electroporation into cells, the non-replicating JFH1 strain (genotype 2a) SGRm-JFH1BlaRL/GND RNA was degraded rapidly in the first 12 h, followed by a further slow decay in the next 9 h, when the luciferase activity dropped to background level. There was no appreciable difference among 7.5-Bsr, 7.5-ISG20 and 7.5-ISG20m cells (Fig. 3B). Similar results were obtained when the replication-incompetent NmLuc/ΔGDD RNA (HCV-N strain, genotype 1b) was used in lieu of SGRm-JFH1BlaRL/GND RNA (Fig. 3C). These data indicate that ISG20 does not seem to accelerate the degradation of transfected HCV RNAs.

Translation of the positive-sense HCV RNA is directed by an IRES within HCV 5′NTR, and leads to synthesis of viral proteins required for HCV replication. We considered the possibility that ISG20 may exert

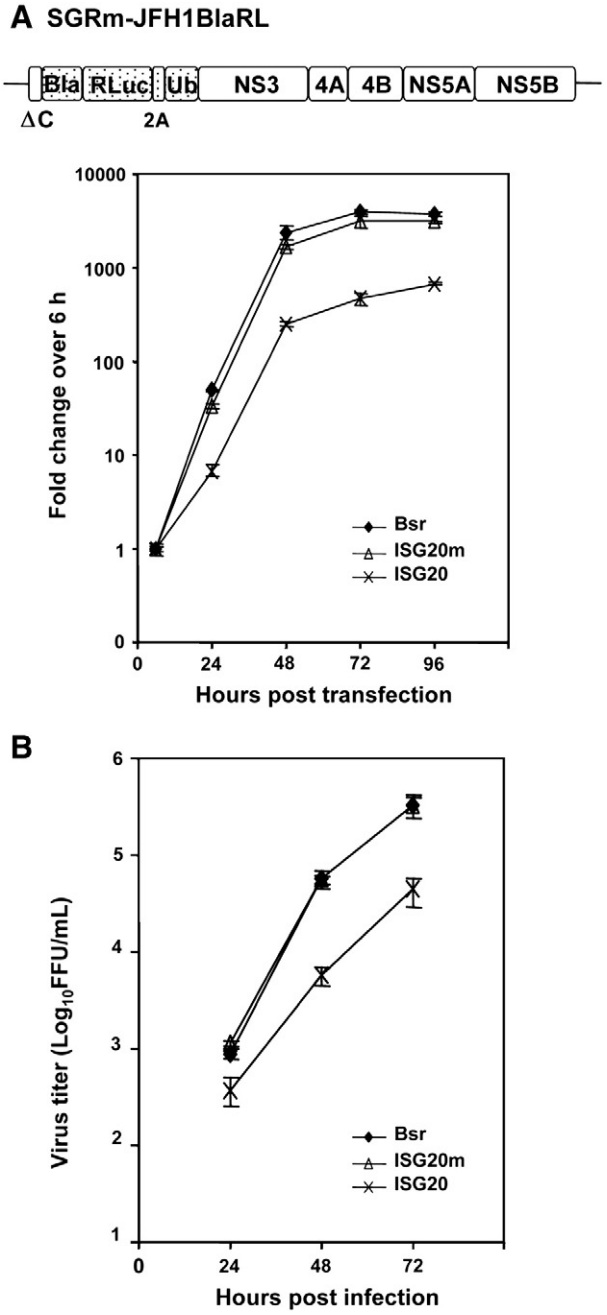

Fig. 2. ISG20 inhibits the replication of subgenomic JFH1 replicon and propagation of cell culture derived JFH1 virus. (A) Upper panel, schematic representation of the monocistronic, renilla luciferase (RLuc) encoding subgenomic replicon, SGRm-JFH1BlaRL. The structural genes of JFH1, core-E1-E2-p7-NS2, were removed and substituted with blasticidin S deaminase (Bla)—RLuc fusion gene, followed by foot and mouse disease virus 2A autoprotease peptide and ubiquitin, which direct the processing of the N-terminus of NS3. Lower panel, 7.5-Bsr, 7.5-ISG20, and 7.5-ISG20m cells were transfected with SGRm-JFH1RL replicon RNA and harvested at indicated time points for RLuc assay. The data shown represent the fold-increase in RLuc activity over that present at 6 h in each cell type, and are representative of at least 3 independently conducted experiments. (B) 7.5-Bsr, 7.5-ISG20, and 7.5-ISG20m cells were infected with JFH1 virus at an MOI = 0.05. At indicated time points, cell-free culture supernatants were harvested and subject to infectious virus titer determination by fluorescent focus forming assay in naïve Huh7.5 cells. Data shown are representative of at least two independently conducted experiments.

its antiviral effect by inhibiting IRES-mediated translation. To test this, we transfected 7.5-Bsr, 7.5-ISG20 and 7.5-ISG20m cells with pRL-HL (Lerat et al., 2000), a dicistronic reporter vector expressing renilla luciferase by cap-dependent translation, and a downstream firefly luciferase coding sequence under cap-independent control of the HCV IRES (Fig. 3D). As shown in Fig. 3E, both cap-dependent and HCV IRES-dependent translation efficiencies were comparable among the three different cell populations, indicating that the antiviral action of ISG20 against HCV replication does not result from any effect on HCV IRES activity.

ISG20m exerts dominant negative (DN) effect on the antiviral action of IFN against intracellular HCV RNA replication

ISG20m exhibited a DN effect on the activity of endogenous ISG20 against VSV infection in HeLa cells (Espert et al., 2003). In contrast, we did not observe increased permissiveness for JFH1 virus RNA replication (Fig. 2A) or JFH1 infection (Fig. 2B) when comparing 7.5-ISG20m and 7.5-Bsr cells. This lack of DN effect of ISG20m was most likely due to the absence of detectable basal ISG20 protein expression in Huh7.5 derived cells (Fig. 1B, lower panel). To determine whether ISG20m inhibits the anti-HCV activity of IFN (which induces ISG20 expression), we pretreated 7.5-Bsr and 7.5-ISG20m cells with a high concentration of human IFN-α (1000 U/ml) to induce a cellular antiviral state. IFN was then removed and cells were transfected with SGRm-JFH1BlaRL replicon RNA to determine the kinetics of intracellular HCV RNA replication (Fig. 4A). In the absence of IFN pretreatment, both 7.5-Bsr and 7.5-ISG20m cells supported robust HCV RNA replication, which reached plateau at 48–72 h posttransfection. There was no appreciable difference between the two cell populations. IFN pretreatment strongly suppressed SGRm-JFH1BlaRL RNA replication in both 7.5-Bsr and 7.5-ISG20m cells, but was substantially less effective in 7.5-ISG20m cells than in 7.5-Bsr cells. At 48 and 72 h posttransfection, HCV RNA replication was reduced by IFN pretreatment by 427-fold and 68-fold, respectively, in 7.5-Bsr cells, but was only decreased by 91-fold and 16-fold, respectively in 7.5-ISG20m cells (Fig. 4A). This difference could not be attributed to an impaired response through Jak-STAT signaling to IFN in 7.5-ISG20m cells, as IFN induction of two well-characterized ISGs, ISG56 and MxA, was of similar efficiency in 7.5-ISG20m cells compared with 7.5-Bsr cells (Fig. 4C). In aggregate, these data suggest that ISG20 is a significant contributor to the IFN antiviral action against intracellular HCV RNA replication, and that this is inhibited by ISG20m.

Next, we determined how ISG20m affects IFN's anti-HCV action in the context of JFH1 virus infection. Towards this end, we pretreated 7.5-Bsr and 7.5-ISG20m cells with a range of IFN-α concentrations (0, 5, 10, 25 and 100 U/ml) to induce a cellular antiviral state. IFN was then removed and cells were infected with JFH1 virus at an MOI of 0.05. At 48 h postinfection, culture supernatants were examined for infectious progeny virus yields by FFU assay (Fig. 4B). We found that pretreatment of cells with as low as 5 U/ml of IFN-α was able to reduce infectious JFH1 virus production by 40%, with no obvious further reduction at higher IFN concentrations. Of note, the reduction of progeny virus yields by IFN pretreatment did not differ between 7.5-Bsr and 7.5-ISG20m cells, regardless of the IFN concentrations used. This suggests that ISG20 mediated inhibition of intracellular HCV RNA replication represents only a fraction of IFN's effects against HCV infection. Conceivably, IFN may also target various steps in HCV life cycle other than intracellular HCV RNA replication, such as viral entry, uncoating, packaging and release, etc (Stark et al., 1998), which may not be targeted by ISG20's exonuclease activity. Such antiviral mechanisms may not be competed by the ectopically expressed ISG20m.

ISG20L1 and ISG20L2 do not inhibit HCV replication

ISG20L1 and ISG20L2 are the two most closely related members to ISG20 in the REX4 gene subfamily within the DEDDh exonuclease family (Coute et al., 2008; Lee et al., 2005). Both proteins have an ExoIII exonuclease domain highly similar to that of ISG20 within their C-terminal portions (Fig. 5A). However, unlike ISG20 which is only composed of an ExoIII domain, ISG20L1 and ISG20L2 have additional

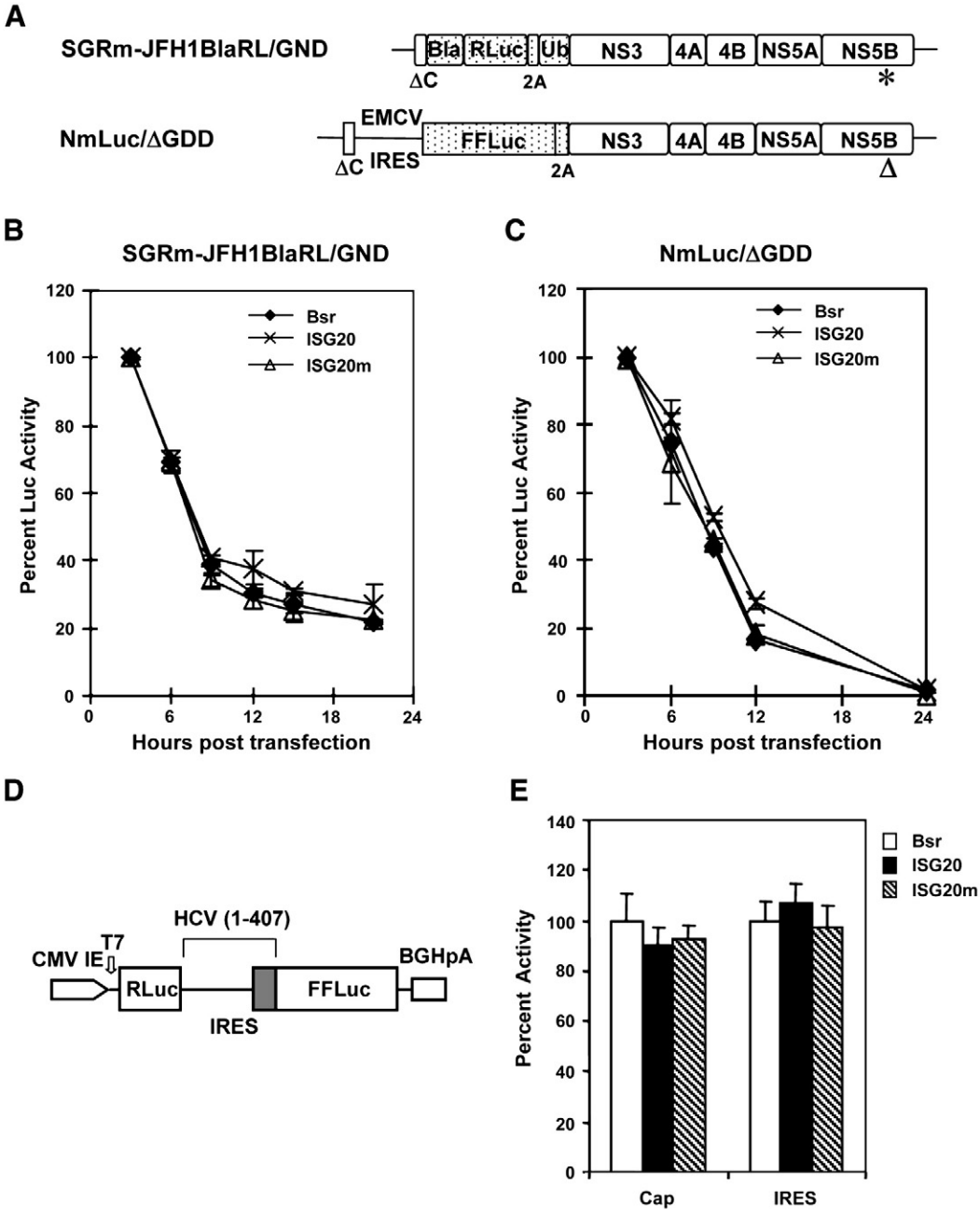

Fig. 3. ISG20 does not accelerate the degradation of transfected HCV RNAs, nor does it inhibit HCV IRES-directed translation. (A) Schematic representation of the replication-incompetent, luciferase-encoding, subgenomic HCV RNAs derived from JFH1 (SGRm-JFH1BlaRL/GND) and HCV-N (NmLuc/ΔGDD) sequences. SGRm-JFH1BlaRL/GND is identical to SGRm-JFH1BlaRL (Fig. 2A) except for the aa mutation in the GDD motif (to GND) in NS5B (indicated by "*"). In NmLuc/ΔGDD, the GDD motif in NS5B is deleted (indicated by "Δ"). Translation of Firefly luciferase (FFLuc), FMDA 2A autoprotease and the downstream NS3 to NS5B polyprotein is directed by EMCV IRES. (B) and (C) 7.5-Bsr, 7.5-ISG20 and 7.5-ISG20m cells were transfected with in vitro transcribed SGRm-JFH1BlaRL/GND (B) or NmLuc/ΔGDD (C) RNAs. At indicated time points post transfection, cells were lysed and subjected to Renilla (B) or Firefly (C) luciferase activity assays. HCV RNA degradation is reflected in the percent decrease in luciferase activity (normalized to that at 3 h post-transfection, when luciferase activity results from translation of initial input HCV RNA). (D) Schematic showing the organization of the bicistronic reporter construct, pRL-HL. CMV-IE: CMV immediate early promoter; BGHpA: bovine growth hormone polyadenylation signal. (E) 7.5-Bsr, 7.5-ISG20, and 7.5-ISG20m cells in triplicate wells were transfected with pRL-HL for 24 h and then lysed for dual luciferase assay determining the translation efficiencies directed by 5′cap (RLuc) and HCV IRES (FFLuc), respectively. Results are normalized to the luciferase activity from transfected Bsr cells (100%).

N-terminal sequences of 108 and 177 aa, respectively. The function of the N-terminal part of ISG20L1 and ISG20L2 is poorly understood, but could determine the predominant nuclear localization of these two proteins (Coute et al., 2008; Lee et al., 2005). In agreement with these previous studies, we found that both ISG20L1 and ISG20L2 were expressed exclusively within the nucleus of transfected Huh7.5 cells, resembling a nuclear body localization pattern (Fig. 5B). To determine whether these two ISG20-like proteins have antiviral activity against HCV, we attempted to establish Huh7.5 cells stably expressing ISG20L1 and ISG20L2, respectively, using retroviral mediated gene transfer. We were able to generate stable Huh7.5 pools expressing ISG20L1 (Fig. 5C). However, efforts to obtain ISG20L2 expressing cells have been unsuccessful thus far—virtually no cells survived the selection process after infection of ISG20L2-encoding retroviruses. The reason for this failure remains unclear, but could reflect cellular toxicity associated with long-term ectopic expression of ISG20L2.

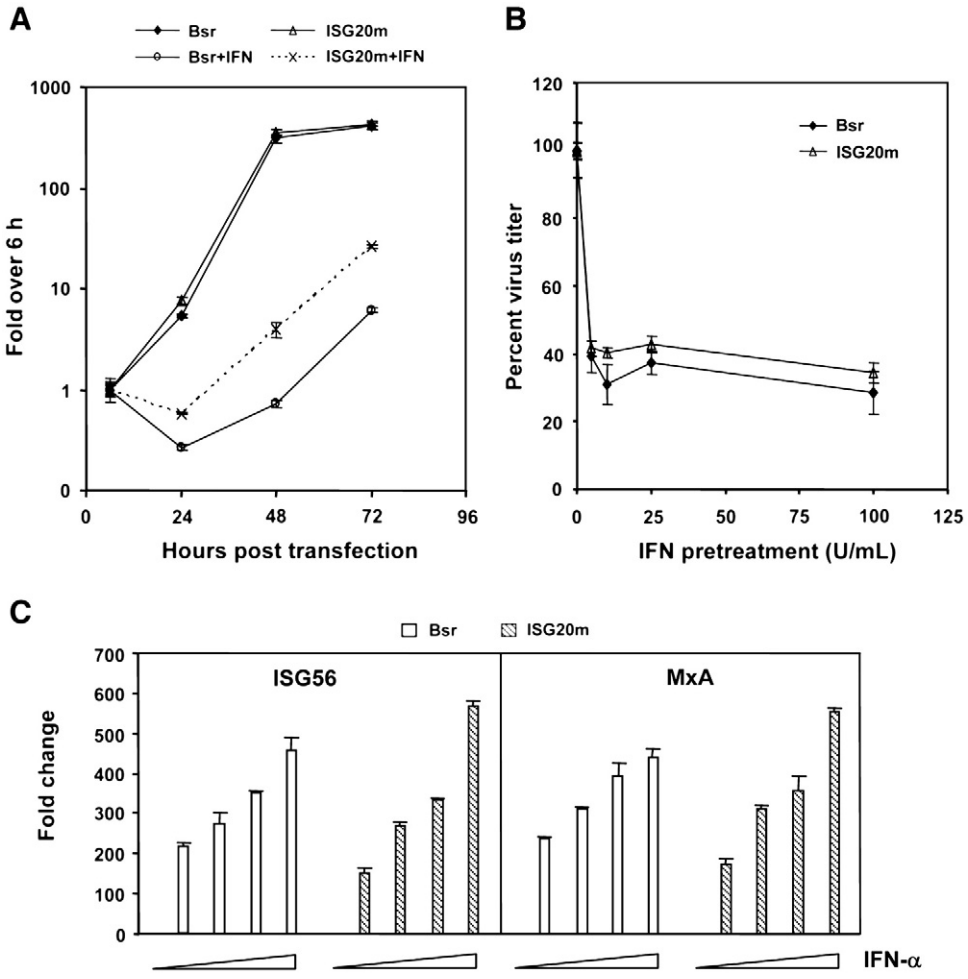

Fig. 4. The exonuclease-deficient ISG20 mutant inhibits the antiviral action of IFN against intracellular HCV RNA replication. (A) 7.5-Bsr and 7.5-ISG20m cells were mock-treated or pretreated with 1000 U/mL of recombinant human IFN-α for 18 h. IFN was then removed and cells transfected with SGRm-JFH1RL replicon RNA. Replication kinetics was analyzed the same way as in Fig. 2A. Data shown were representative of three independent experiments. (B) Triplicate wells of 7.5-Bsr and 7.5-ISG20m cells were pretreated with 0, 5, 10, 25 and 100 U/mL of IFN-α for 24 h. After removal of IFN, cells were infected with JFH1 virus at an MOI = 0.05. Cell free culture supernatants were harvested at 48 h postinfection and infectious virus titer determined by fluorescent focus forming assay. Data are presented as percentage of virus titer relative to cells treated with 0 U/mL IFN. Data are representative of 2 independently conducted experiments. (C) 7.5-Bsr and 7.5-ISG20m cells respond similarly to IFN. Cells were treated with 0, 10, 50, 100, and 1000 U/mL of IFN-α for 7 h prior to total RNA extraction and realtime PCR analysis of ISG56 and MxA mRNA expression. Fold change of each gene was calculated by normalizing the data to 7.5-Bsr mock treated cells (there was no difference in the baselines of ISG56 and MxA mRNAs between mock-treated 7.5-bsr and 7.5-ISG20m cells).

In contrast to its impaired replication ability in 7.5-ISG20 cells, the SGRm-JFH1BlaRL replicon replicated efficiently in 7.5-ISG20L1 cells as it did in 7.5-Bsr cells (Fig. 5D). In agreement with this, intracellular core protein accumulation after JFH1 virus infection was greatly reduced in 7.5-ISG20 cells compared with that in 7.5-Bsr and 7.5-ISG20L1 cells, but was comparable between the latter two (Fig. 5E). Thus, unlike ISG20, ISG20L1 does not have antiviral activity against HCV in cultured hepatoma cells.

Because we were unable to generate stable cells expressing ISG20L2, we adopted a transient co-transfection strategy in determining the effect of ISG20L2 on HCV RNA replication. We co-transfected Huh7 cells with the SGRm-JFH1BlaRL replicon RNA and the ISG20L2 encoding plasmid at a ratio of 1:6 and monitored HCV RNA replication by determining the fold increase in luciferase activity at 72 h over at 6 h post-transfection. As controls, cells were co-transfected with the replicon RNA and ISG20-encoding plasmid (as a positive control) or an empty vector, or the ISG20L1 encoding vector (as negative controls). Although ISG20 strongly inhibited SGRm-JFH1BlaRL replication compared with the empty vector, ISG20L2 and ISG20L1 did not (Fig. 5F). Together, the antiviral activity of ISG20 against HCV is not shared with the closely related proteins, ISG20L1 and ISG20L2.

Fig. 5. ISG20L1 and ISG20L2 do not inhibit HCV replication. (A) Amino acid sequence alignment of the ExoIII domains of ISG20, ISG20L1 and ISG20L2. Numbers shown on the left side of the sequences indicate amino acid positions. The three exonuclease motifs (I, II and III) are marked by top braces. The identical residues throughout the three sequences are in heavy grey-shaded letters, while the semi-identical residues are in light grey-shaded letters. The five conserved amino acid residues (D, E, D, D and H) characteristic of the DEDDh exonuclease superfamily are in black-shaded letters. The ExoIII domain amino acid identities between ISG20 and ISG20L1, ISG20 and ISG20L2 are 57% and 51%, respectively. (B) Subcellular localizations of ISG20L1 and ISG20L2 in transiently transfected Huh7.5 cells. ISG20L1 and ISG20L2 were immunostained green using anti-myc mAb, while nuclei were counterstained blue by DAPI. ISG20L1 showed a similar localization pattern in 7.5-ISG20L1 cells (data not shown). (C) Immunoblot analysis of ISG20L1 (using anti-myc mAb) and actin expression in 7.5-bsr (lane 1) and 7.5-ISG20L1 (lane 2) cells. (D) Replication kinetics of SGRm-JFH1RL replicon in 7.5-Bsr, 7.5-ISG20, and 7.5-ISG20L1 cell. Cells were transfected and analyzed similarly to Fig. 2A. Data shown are representative of two independently conducted experiments. (E) 7.5-Bsr, 7.5-ISG20, and 7.5-ISG20L1 cells were infected with JFH1 virus at an MOI of 0.05. At indicated time points, cell lysates were subject to immunoblot analysis of HCV core and actin expression. Results are representative of 2 independently conducted experiments. (F) Huh7 cells were transiently co-transfected with SGRm-JFH1BlaRL replicon RNA and an empty vector or plasmid encoding ISG20, ISG20L1, or ISG20L2, respectively, at a ratio of 1:6 using lipofectamine 2000. Replication of SGRm-JFH1RL replicon was determined by calculating the fold increase of luciferase activities at 72 h over those at 6 h posttransfection (upper panel). In lower panel, expression of ISG20, ISG20L1 and ISG20L2 proteins were analyzed by western blot using anti-myc mAb. Actin was immunoblotted to demonstrate equal sample loading.

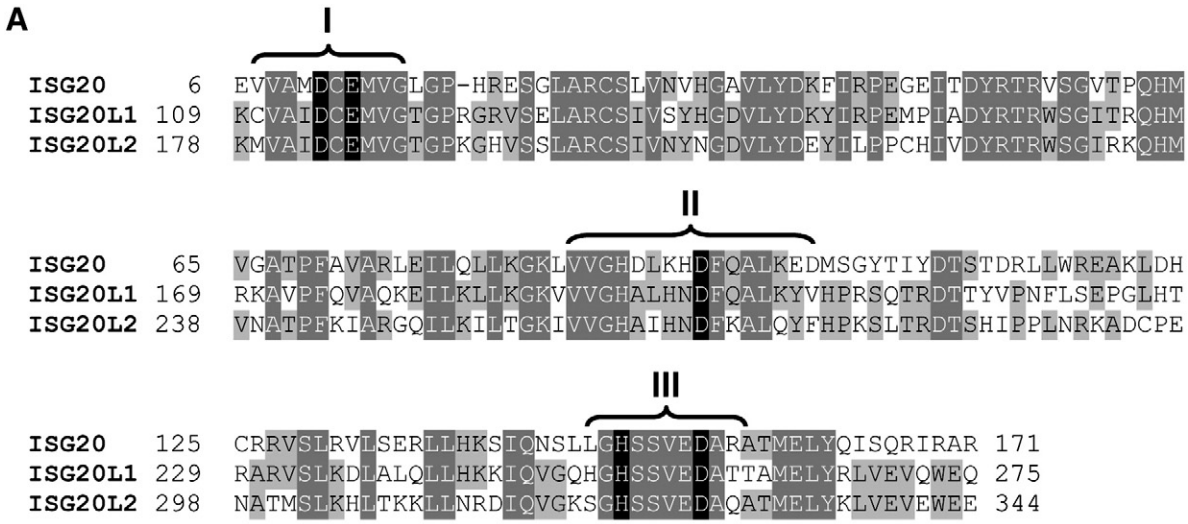
A
I
II
III
ISG20 6 EVVAMDCEMVGLGP-HRESGLARCSLVNVHCAVLYDKFIRPEGEITDYRTRVSGVTPQHM
ISG20L1 109 KCVAIDCEMVGTGPRGRVSELARCSIVSYHGDVLYDKYIRPEMPIADYRTRWSGITRQHM
ISG20L2 178 KMVAIDCEMVGTGPKGHVSSLARCSIVNYNGDVLYDEYILPPCHIVDYRTRWSGIRKQHM
ISG20 65 VGATPFAVARLEILQLLKGKLVVGHDLKHDFQALKEDMSGYTIYDTSTDRLLWREAKLDH
ISG20L1 169 RKAVPFQVAQKEILKLLKGKVVVGHALHNDFQALKYVHPRSQTRDTTYVPNFLSEPGLHT
ISG20L2 238 VNATPFKIARGQILKILTGKIVVGHAIHNDFKALQYFHPKSLTRDTSHIPPLNRKADCPE
ISG20 125 CRRVSLRVLSERLLHKSIQNSLLGHSSVEDARATMELYQISQRIRAR 171
ISG20L1 229 RARVSLKDLALQLLHKKIQVGQHGHSSVEDATTAMELYRLVEVQWEQ 275
ISG20L2 298 NATMSLKHLTKKLLNRDIQVGKSGHSSVEDAQATMELYKLVEVEWEE 344

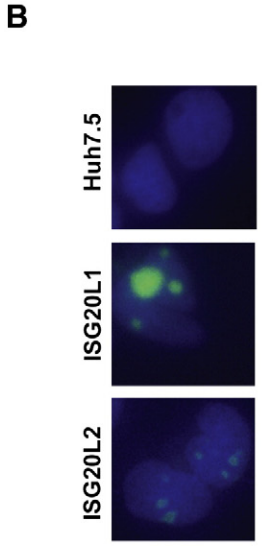
B
Huh7.5
ISG20L1
ISG20L2

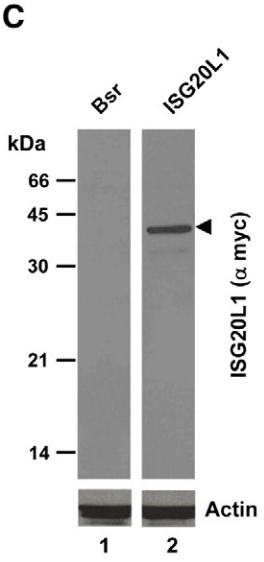
C
Bsr
ISG20L1
kDa
66
45
30
21
14
ISG20L1 (α myc)
Actin
1
2

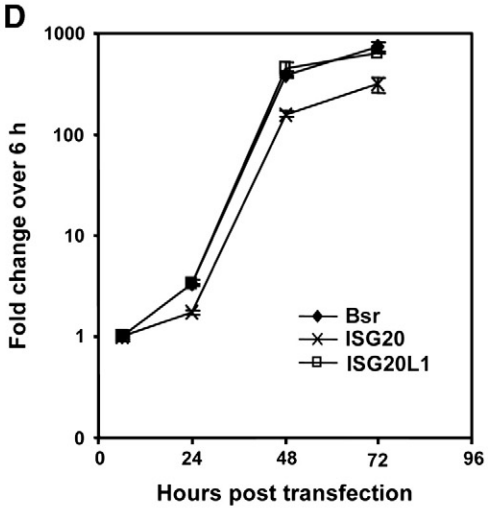
D
Fold change over 6 h
1000
100
10
1
0
0
24
48
72
96
Hours post transfection
Bsr
ISG20
ISG20L1

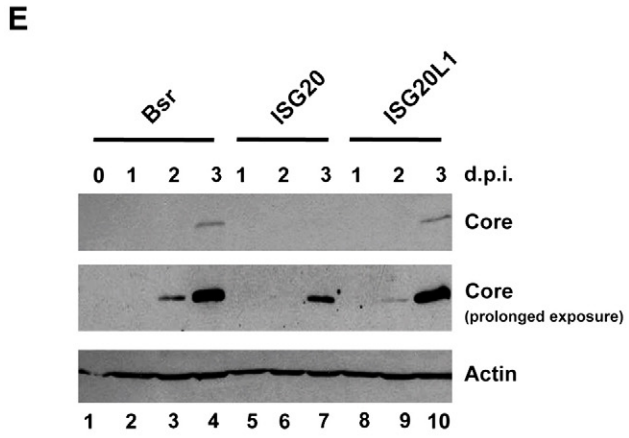
E
Bsr
ISG20
ISG20L1
0 1 2 3 1 2 3 1 2 3 d.p.i.
Core
Core
(prolonged exposure)
Actin
1 2 3 4 5 6 7 8 9 10

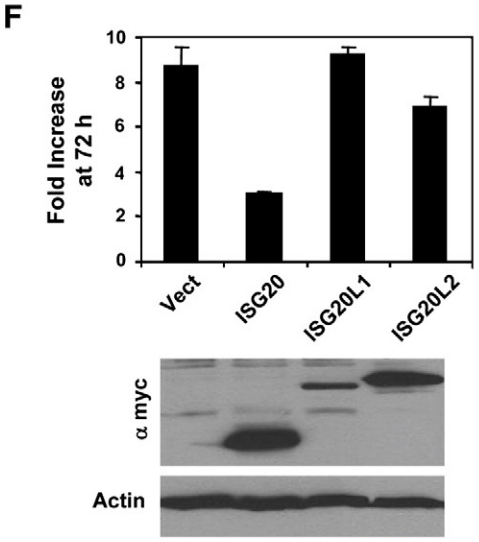
F
Fold Increase
at 72 h
10
8
6
4
2
0
Vect
ISG20
ISG20L1
ISG20L2
α myc
Actin

ISG20 inhibits BVDV infection in bovine kidney cells

Classified within the genus *pestivirus* in the family *Flaviviridae*, BVDV shares similar genome structure and replication strategy with HCV. It has been the most widely used in vitro surrogate model system for the identification and characterization of antiviral agents for use against HCV (Buckwold et al., 2003) before the HCV cell culture system became available. Since ISG20 suppresses HCV RNA replication, we asked the question whether replication of the closely related BVDV is also subject to the inhibitory action of ISG20. Toward this end, we established MBDK cell pools stably expressing ISG20 (designated as BK-ISG20), ISG20m (designated as BK-ISG20m) and the control vector (designated as BK-Bsr), respectively, by retroviral mediated gene transfer. In contrast to the control BK-Bsr cells, BK-ISG20 and BK-ISG20m cells expressed abundant myc-tagged ISG20 or ISG20m protein (Figs. 6A and B), which demonstrated both cytoplasmic and

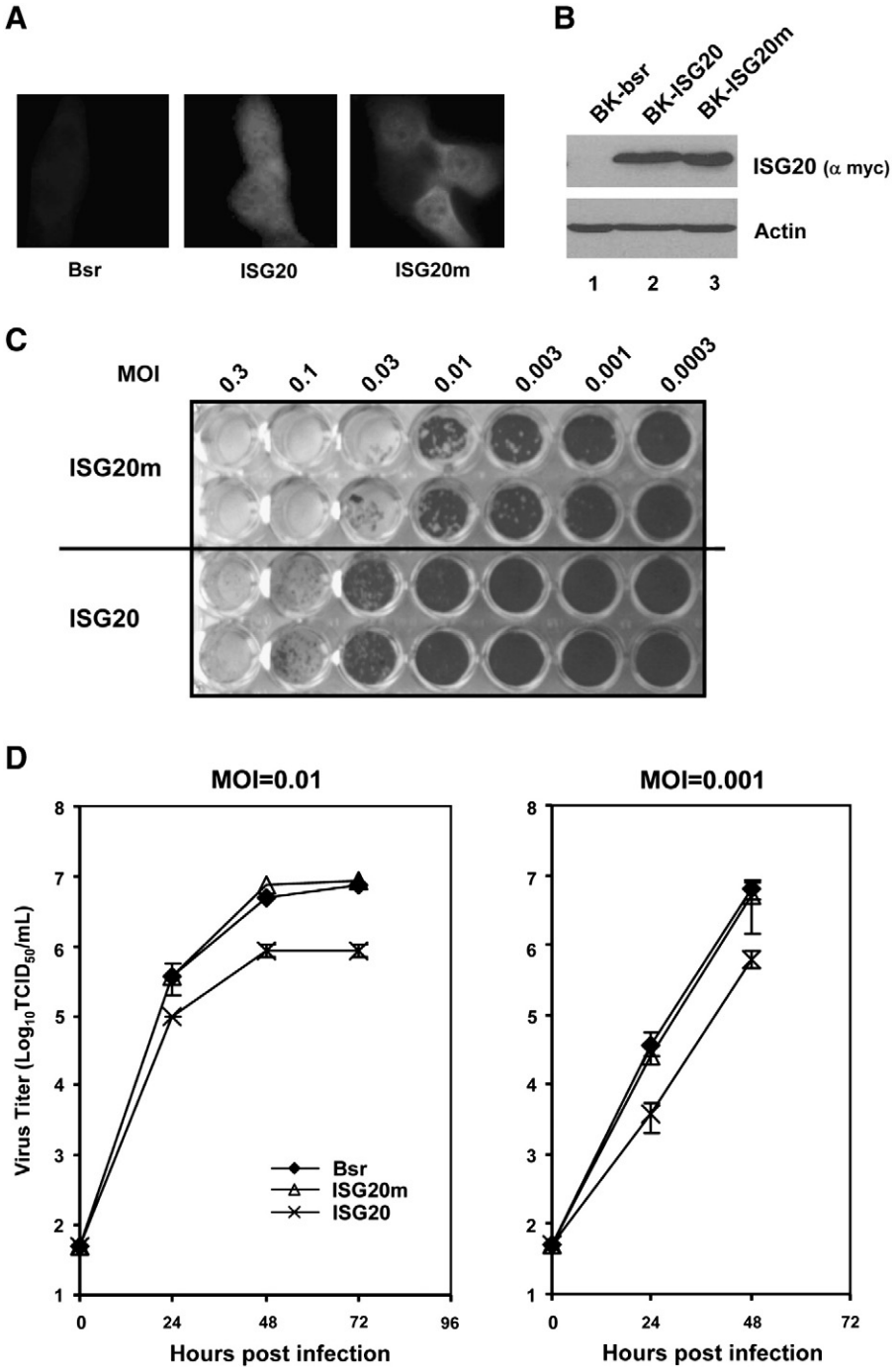

Fig. 6. ISG20 inhibits BVDV infection in MDBK cells. (A) Immunostaining of ISG20/ISG20m expression using anti-myc tag mAb in BK-Bsr (left), BK-ISG20 (middle) and BK-ISG20m (right) cells. (B) Upper panel, immunoblot analysis of ISG20 and ISG20m expression (using anti-myc tag mAb) in BK-Bsr, BK-ISG20 and BK-ISG20m cells. In lower panel, beta-actin was blotted to show equal sample loading (C). Duplicate wells of BK-ISG20m (upper two rows) and BK-ISG20 (lower two rows) cells grown in a 96-well plate were infected with increasing MOIs (from right to left, 0.0003 through 0.3) of the cytopathic NADL strain of BVDV for 66 h prior to cell fixation and crystal violet staining. Image shown is representative of two independently conducted experiments. (D) BK-bsr, BK-ISG20 and BK-ISG20m cells were infected with BVDV NADL at an MOI of 0.01 (left) or 0.001 (right). At the indicated time points, cell-free culture supernatants were harvested and viral titers were determined by $TCID_{50}$ assay on naïve MDBK cells. Data shown are representative of two independently conducted experiments.

nuclear localization (Fig. 6A), a pattern similar to that observed for ISG20 in human cells (Fig. 1A) (Espert et al., 2003, 2006). When infected with the cytopathic BVDV NADL virus at a range of increasing MOIs (0.0003 to 0.3), BK-ISG20 cells had substantially less CPE and more cell survival than did BK-ISG20m cells (Fig. 6C). In agreement with this, progeny BVDV yields from infected BK-ISG20 cells were consistently about 1-log lower than those in BK-Bsr and BK-ISG20m cells at 48 and 72 h postinfection, with the latter two being similar (MOI = 0.01 and 0.001, shown in Fig. 6D). We conclude from these experiments that similar to HCV, BVDV is also sensitive to the antiviral action of ISG20 in cell culture.

Cell-type specific antiviral effect of ISG20 against YFV infection

Next, we determined how ISG20 affects the replication of YFV, a prototype member of the genus *flavivirus* in the family *Flaviviridae*. When infected with the virulent Asibi strain of YFV (MOI = 0.1), all three Huh7.5 derived cells supported efficient virus growth. There were no appreciable differences in infectious progeny virus release (Fig. 7A) and intracellular accumulation of YFV NS3 antigen (Fig. 7B) in the 3- to 4-day observation period, regardless of ISG20/ISG0m expression status. The results did not differ when the vaccine strain (17D) of YFV was used in lieu of Asibi strain for the infection (Fig. 7C). Thus, in contrast to its effect on HCV, ISG20 does not inhibit YFV propagation in hepatoma Huh7.5 cells.

To determine whether the lack of antiviral activity against YFV by ISG20 in huh7.5 cells was a cell-type specific phenomenon, we took advantage of HEK293 FLP-IN T-Rex cells with tet-regulated conditional expression of ISG20 or ISG20m (Jiang et al., 2008). Cells were cultured to induce (+tet) or repress (−tet) ISG20 or ISG20m expression, followed by infection with YFV-17D virus (MOI = 0.1) for 4 days. YFV-17D grew at a much slower rate in HEK293 cells than it

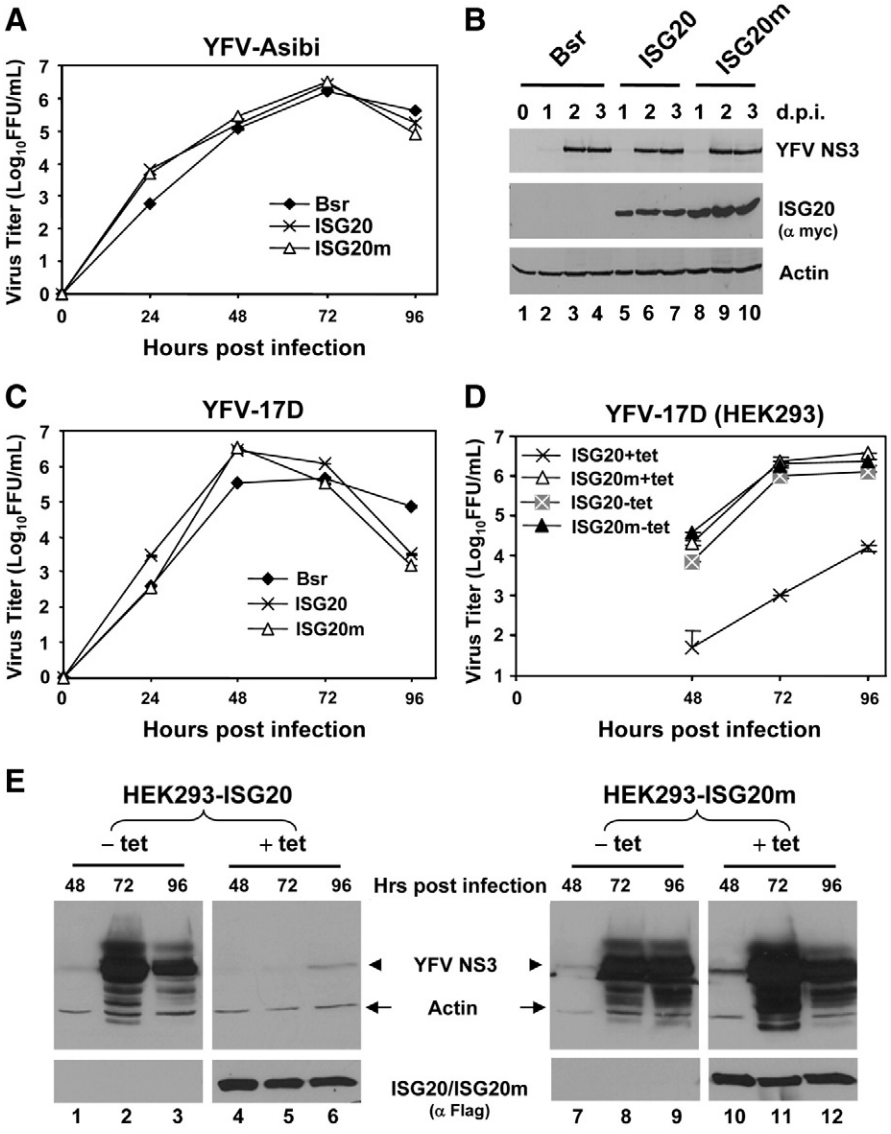

Fig. 7. Cell-type specific antiviral effect of ISG20 against YFV infection. 7.5-Bsr, 7.5-ISG20 and 7.5-ISG20m cells were infected with YFV Asibi strain (MOI = 0.1) (panels A and B) or YFV 17D strain (MOI = 0.1) (panel C). At indicated time points, cell-free culture supernatants were harvested and viral titers determined by fluorescent focus-forming assay (panels A and C). Data shown were representative of two independently conducted experiments. (B) Immunoblot analysis of YFV NS3, ISG20 (using anti-myc antibody), and actin expression in cell lysates under conditions in panel A. (D) HEK293-FLP-IN T-Rex cells that conditionally express ISG20 or ISG20m were cultured in the presence or absence of 1 μg/ml tetracycline for 2 days, to induce or repress ISG20/ISG20m expression, respectively, and subsequently infected with YFV 17D virus (MOI = 0.1) for 4 days. Cell-free culture supernatants were harvested and progeny viral titers were determined by fluorescent focus-forming assay (panel D). Cell lysates were harvested and subjected to immunoblot analysis of YFV NS3 (arrow head), actin (arrow) and ISG20/ISG20m (using anti-Flag antibody) proteins (panel E). Data shown are representative of two independently conducted experiments.

did in Huh7.5-derived cells, with progeny virus in culture supernatant first detected at 48 h post-infection (Fig. 7D). We found that induction of ISG20, but not ISG20m, reduced progeny YFV production by 2–3 logs at 48 to 96 h post-infection (Fig. 7D). Consistent with this, accumulation of YFV NS3 antigen was diminished in HEK293 cells expressing ISG20 (Fig. 7E, compare lanes 5 and 6 vs 2 and 3) but not in cells induced for ISG20m expression (Fig. 7E, compare lanes 11 and 12 vs 8 and 9). Collectively, although ISG20 has no demonstrable antiviral activity against YFV in Huh7.5-derived cells, it potently inhibits YFV replication in HEK293 cells and such an effect depends on its catalytic activity.

ISG20 inhibits HAV replication

HAV is a picornavirus that infects mainly hepatocytes, causing acute hepatitis in vivo (Martin and Lemon, 2006). To determine whether ISG20 inhibits HAV replication, we first compared the replication efficiency of a subgenomic HAV RNA replicon encoding luciferse (HAV-Luc, Fig. 8A) among 7.5-Bsr, 7.5-ISG20, and 7.5-ISG20m cells. HAV-Luc replicated efficiently in both 7.5-Bsr and 7.5-ISG20m cells with similar kinetics, resulting in an increase in luciferase activity over 72 h followed by a plateau later. In contrast, replication of HAV-Luc was substantially compromised in 7.5-ISG20 cells, resulting 5- to 7-fold lower luciferase activity than that observed with 7.5-Bsr and 7.5-ISG20m cells 72–96 h posttransfection (Fig. 8B). These results suggest that ISG20 expression restricts HAV RNA replication in Huh7.5 cells. To determine whether ISG20 inhibits HAV replication in the context of virus infection, HEK293 FLP-IN T-Rex cells with tet-regulated expression of ISG20 or ISG20m were cultured to induce (+tet) or repress (−tet) ISG20 or ISG20m expression (Fig. 8C), followed by infection with HAV-18f virus for 5 days. Induction of ISG20 was associated with a reproducible, 2-fold reduction in progeny HAV yield, while no such effect was observed upon ISG20m expression (Fig. 8D). Collectively, ISG20 inhibits HAV replication in both hepatic and non-hepatic cells and the anti-HAV effect is dependent on the exonuclease activity of ISG20.

ISG20 does not inhibit propagation of SARS-CoV in Huh7.5 cells

SARS-CoV is a highly pathogenic human coronavirus which was just recognized in 2003. Unlike other known human coronaviruses which are usually associated with mild upper respiratory tract infection, infection with SARS-CoV causes severe lower respiratory illness with a mortality rate of ~10% (Peiris et al., 2004, 2003). Although there is no specific antiviral therapy available for treatment of SARS, IFN is known to inhibit SARS-CoV replication in vitro and protect against SARS-CoV infection in vivo (Cinatl et al., 2003; Haagmans et al., 2004; Spiegel et al., 2004; Zheng et al., 2004). Since ISG20 was highly upregulated in lungs of cynomolgus macaques experimentally infected with SARS-CoV (de Lang et al., 2007), we set out to determine whether ISG20 contributes to the antiviral action of IFN against SARS-CoV, taking advantage of the fact that SARS-CoV

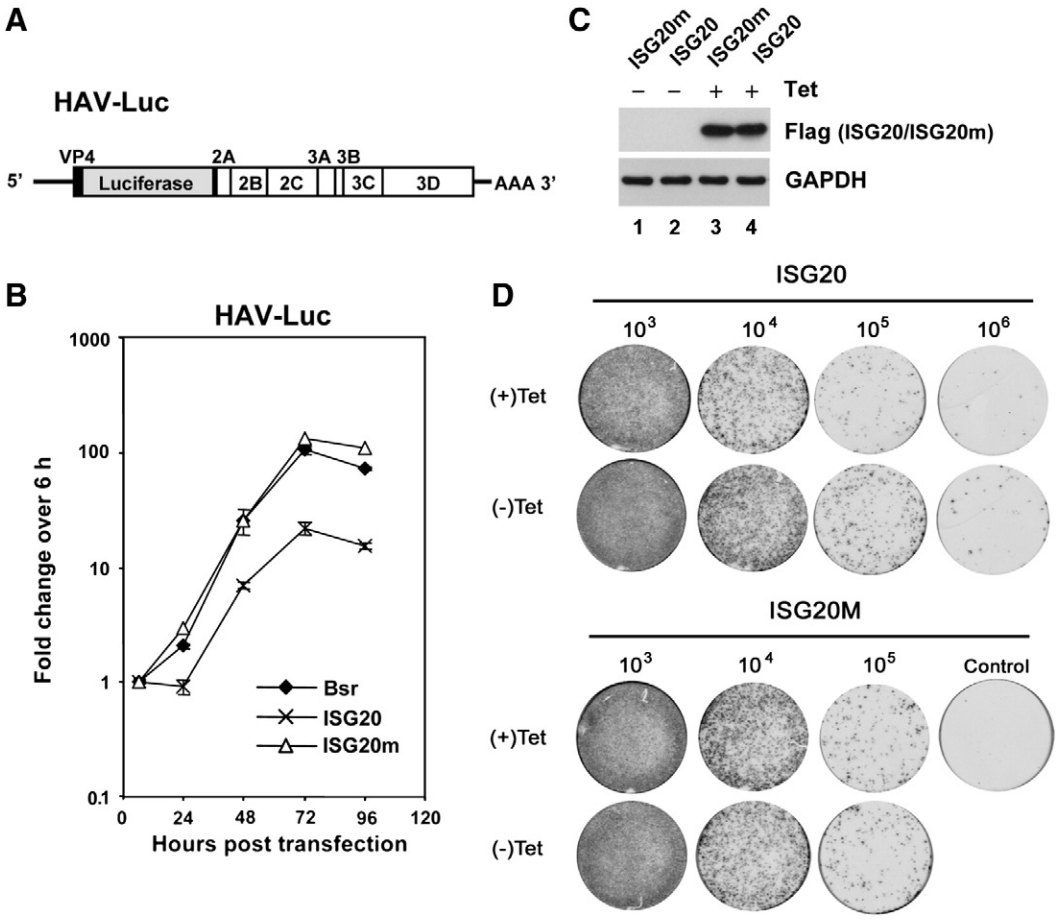

Fig. 8. ISG20 inhibits HAV replication. (A) Schematic representation of the HAV-Luc replicon (Yi et al., 2002). (B) Replication kinetics of HAV-luc replicon in 7.5-Bsr, 7.5-ISG20 and 7.5-ISG20m cells. Data shown are representative of 3 independent experiments. (C and D) HEK293-FLP-IN T-Rex cells that conditionally express ISG20 or ISG20m were cultured in the presence or absence of 2 μg/ml tetracycline for 3 days, to induce or repress ISG20/ISG20m expression, respectively, and subsequently infected with HM175/18f virus (MOI = 1) for 5 days. Then cell lysates were harvested and immunoblotted for expression of ISG20/ISG20m (using anti-Flag antibody) and GAPDH (panel C), and HAV infectious virus yield was determined by infrared fluorescent immunofocus assay of 10-fold serially diluted samples on FRhK-4 cells (panel D). In panel D, the control dish in ISG20m (+tet) at 10^6 dilution was stained with secondary antibody conjugate only.

replicates in Huh7 cells (Devaraj et al., 2007; Hattermann et al., 2005; Tang et al., 2005). When infected at a low MOI (0.01), 7.5-Bsr, 7.5-ISG20 and 7.5-ISG20m cells released similar amount of progeny viruses in culture medium at all time points during the 3-day observation period (Fig. 9A). Consistent with this, intracellular accumulation of SARS-CoV nucleocapsid protein was comparable among these cell populations, regardless of the ISG20/ISG20m expression status (Fig. 9B). These data reveal that ISG20 does not inhibit SARS-CoV replication in hepatoma Huh7.5 cells.

Discussion

In this study, we have characterized the antiviral spectrum of ISG20 in vitro by determining the effects of ectopically expressed ISG20 on replication of a number of distinct positive strand RNA viruses. Previously, it has been shown that ISG20 exhibits antiviral activity against vesicular stomatitis virus, EMCV, influenza virus, HIV, and Sindbis virus (Espert et al., 2003, 2005; Zhang et al., 2007). It is demonstrated in the current study that ISG20 also inhibits HAV, BVDV and cell culture derived HCV (JFH1 virus). Furthermore, we report that ISG20 exhibits cell-type specific antiviral activity against YFV infection (Fig. 7)—while ISG20 had no demonstrable anti-YFV effect in Huh7.5-derived cells, it potently inhibited YFV replication in HEK293 cells. The latter result is in line with a very recent report which demonstrated that ISG20 inhibited infections by two closely related flaviviruses to YFV, West Nile virus and Dengue virus, when ectopically expressed in HEK293 cells (Jiang et al., 2010). At present, we do not know what cellular factor(s) contributes to the disparate anti-YFV activity of ISG20 between Huh7.5 and HEK293 cells. Nonetheless, our data suggests the need for caution when interpreting results obtained from different cell types. Thus, although we did not observe an antiviral effect of ISG20 on propagation of SARS-CoV in Huh7.5 cells (Fig. 9), further studies are needed to determine whether this holds true in other cell types that support efficient SARS-CoV replication.

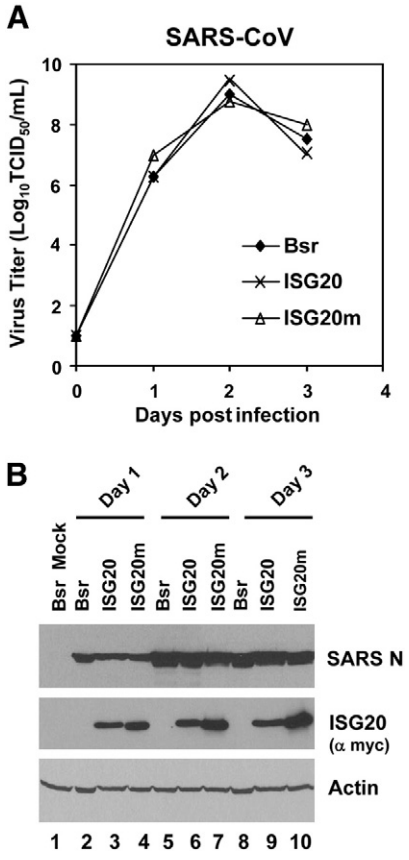

Fig. 9. ISG20 does not inhibit SARS-CoV replication in Huh7.5 cells. (A) 7.5-Bsr, 7.5-ISG20 and 7.5-ISG20m cells were infected with SARS-CoV, Urbani strain (MOI = 0.01). At indicated time points, cell-free culture supernatants were harvested and viral titers determined by TCID50 assay on Vero E6 cells. Data shown were representative of two independently conducted experiments. (B) Immunoblot analysis of SARS-CoV nucleocapsid (N), ISG20/ISG20m (using anti-myc mAb), and actin expression in cell lysates under conditions of panel A.

Recently, ISG20 was reported to inhibit genotype 1b (HCV-N strain) subgenomic HCV RNA replicons when stably expressed in HEK293 cells (Jiang et al., 2008). The current study shows that ISG20 also acts to inhibit the replication of genotype 2a (JFH1) subgenomic replicon as well as propagation of cell culture-derived HCV (JFH1 virus) in cultured hepatocytes. Furthermore, our results show that ectopically expressed ISG20 inhibits HCV RNA replication and progeny virus release in Huh7.5 cells that lack both RIG-I and TLR3 viral RNA sensing pathways which recognize HCV replication and trigger IFN antiviral responses (Li et al., 2005a; Saito et al., 2008; Sumpter et al., 2005; Wang et al., 2009). Therefore, the antiviral action of ISG20 against HCV infection does not seem to depend on an IFN-inducible factor. This is in contrast to what has been shown for the zinc-finger antiviral protein, an ISG that requires an IFN-induced factor to inhibit alphavirus virion production (MacDonald et al., 2007). However, our results do not rule out the possibility that one or more IFN-stimulated cellular factors may enhance the antiviral activity of ISG20.

The demonstrated antiviral activities of ISG20 against HCV, HAV, BVDV and YFV all require the exonuclease activity of ISG20, as they were consistently abrogated by the D94G mutation that specifically disrupts the active site of ISG20 ExoIII domain (Figs. 2, 6–8)(Jiang et al., 2008; Nguyen et al., 2001). The currently proposed effector mechanism of ISG20 involves the degradation of viral RNAs by the 3′–5′ exonuclease activity of ISG20 (Degols et al., 2007). However, precisely how ISG20 acts to inhibit HCV, HAV, YFV and BVDV infection is not known. Our results show that ISG20 does not enhance the degradation of transfected HCV RNA, regardless of the virus strains (JFH1, genotype 2a and HCV-N, genotype 1b) tested (Fig. 3A–C). While this is a little surprising, it is possible that ISG20 exerts its antiviral action by targeting a cellular factor(s) required for virus replication (Degols et al., 2007). However, it is also possible that ISG20 only recognizes HCV RNAs which are associated with replication complex and/or reside in certain cellular compartments. It should be noted that our RNA stability data (Fig. 3A–C) were from replication defective RNAs and hence gave no information on whether ISG20 promotes the degradation of negative strand HCV RNA, which could constitute an antiviral mechanism of ISG20. We show that ISG20 does not affect HCV IRES-mediated translation (Fig. 3E), an essential step before HCV proteins, including the nonstructural proteins involved in viral RNA replication, are made. Furthermore, we demonstrate that ectopically expressed, D94G mutant ISG20 suppresses IFN's antiviral effect on replication of subgenomic HCV RNAs in hepatoma cells (Fig. 4A), indicating that ISG20 is a critical component in executing IFN's antiviral actions against HCV RNA replication in hepatocytes. Conceivably, the catalytically-inactive ISG20 mutant may act as a DN inhibitor that competes with ISG20 in recognizing/associating with the viral/cellular substrate(s). When JFH1 virus was used in probing IFN's antiviral action, the DN effect of the D94G mutant ISG20 was not as evident (Fig. 4B). This is not surprising, as IFN likely targets multiple stages of HCV life cycle which are not recapitulated in the HCV RNA replicon system and are probably not subjected to ISG20's action, such as viral attachment, entry, uncoating, packaging, and egress, etc.

ISG20L1 and ISG20L2 represent the two most closely related 3′ to 5′ exoribonucleases to ISG20 (Coute et al., 2008; Lee et al., 2005). Both share a highly similar EXOIII domain with ISG20, with amino acid identities of 57% (ISG20L1) and 51% (ISG20L2) compared with ISG20, respectively. The biological functions of these two ISG20-like proteins are not well understood. ISG20L1 (a.k.a., AEN) is induced by p53

following ionizing radiation and DNA damage and is required for efficient DNA fragmentation in p53-dependent apoptosis (Lee et al., 2005). ISG20L2 is involved in ribosome biogenesis at the level of 5.8S rRNA maturation, more specifically in the processing of the 12S precursor rRNA (Coute et al., 2008). Our data analyzing HCV RNA replication efficiencies in hepatoma cells ectopically expressing ISG20L1 or ISG20L2 did not reveal an antiviral function of these two ISG20-like proteins, at least against HCV (Fig. 5). While there may be intrinsic differences in substrate preference of ISG20L1 and ISG20L2 from that of ISG20, it is of note that ISG20L1 and ISG20L2 localize within nucleus (Fig. 5B) (Coute et al., 2008; Lee et al., 2005), whereas ISG20 is distributed in both nucleus and cytoplasm (Figs. 1A and 6A) (Espert et al., 2003, 2006). It is possible that ISG20L1 and ISG20L2 do not have access to HCV RNA and/or cellular factors essential for HCV replication, which are targeted by ISG20.

ISG20 mRNA is highly upregulated in liver of chimpanzees infected with HCV or following intravenous administration of IFN (Bigger et al., 2001; Lanford et al., 2006). In the liver of chimpanzees acutely infected with hepatitis B virus (HBV), ISG20 was induced during the viral clearance stage (Wieland et al., 2004). Interestingly, ISG20, when ectopically expressed in HepG2 cells, reduces the secretion of HBs and HBe antigens in transfected HepG2 cells (Hao and Yang, 2008). The broad antiviral activities of ISG20 against multiple, distinct hepatitis viruses (HAV, HCV and HBV) indicate that ISG20 is an important antiviral effector molecule downstream of IFN signaling in innate defenses of the liver.

Materials and methods

Plasmids

Conventional PCR techniques were used to construct retroviral expression vectors encoding human ISG20, ISG20L1 and ISG20L2, respectively, in pCX4Bsr backbone (Akagi et al., 2003). pCX4Bsr-ISG20-myc encodes C-terminal myc-6Xhis tagged human ISG20, while pCX4Bsr-ISG20L1 and pCX4Bsr-ISG20L2 encode C-terminal myc-tagged human ISG20L1 and ISG20L2, respectively. pCX4Bsr-ISG20m-myc contains cDNA sequence encoding the catalytically inactive mutant ISG20. It is different from pCX4Bsr-ISG20-myc in that the codon Asp 94 (GAC) of human ISG20 was converted to Gly (GGC). The bicistronic reporter plasmid pRL-HL and subgenomic pHAV-Luc replicon construct have been described (Lerat et al., 2000; Yi and Lemon, 2002).

The monocistronic pSGRmJFH1BlaRL replicon was constructed as follows. pFL-J6/JFH-5′C19Rluc2AUbi (kindly provided by C. Rice) (Tscherne et al., 2006) was first modified to include blasticidin resistance gene directly fused to the N-terminus of Renilla luciferase. To achieve this, the EcoRI–MluI fragment containing the entire 5′NTR and the first 19 core-coding sequences in pFL-J6/JFH-5′C19Rluc2AUbi was replaced with a similarly digested fragment amplified by PCR from pSGR-JFH1-blast (kindly provided by G. Luo) (Chang et al., 2006) using the primers, EcoRIT7+, cagtgaattctaatacgactcactatag, and MluIBlanostop−, gtcatacgcgtGCCCTCCCACACATAAC. The resulting plasmid was named as pJ6JFH1BlaRL. Subsequently, QuikChange site-directed mutagenesis was conducted to remove the HCV Core-E1-E2-p7-NS2 coding sequences downstream of the ubiquitin sequence, leading to a direct fusion of N-terminus of NS3 to ubiquitin. The resulting plasmid was digested with AgeI and AvrII to release the cDNA fragment (hereafter referred as fragment L) containing partial 5′NTR, the first 12 aa coding sequence of Core, the blasticidin resistance gene, full Renilla luciferase coding sequence, FMDV 2a autoprotease sequence, ubiquitin and partial NS3 coding sequence. pSGR-JFH1 (Kato et al., 2003) (kindly provided by T. Wakita) was digested with AgeI and AvrII to remove the partial 5′NTR, the first 19 aa coding sequence of Core, the neomycin phosphotransferase II gene, EMCV IRES and partial NS3 coding sequence, and used as a vector for ligation with fragment L to generate the monocistronic replicon, pSGRmJFH1BlaRL. A replication defective mutant replicon, pSGRmJFH1BlaRL/GND, was constructed the same way except that pSGR-JFH1/GND was used as the vector backbone for ligation with fragment L. The fragment L in both constructs was fully sequenced to confirm its authenticity. A monocistronic, replication defective mutant replicon of HCV-N strain, NmLuc/ΔGDD, was constructed by replacing the cDNA fragment containing the neomycin phosphotransferase II gene and EMCV IRES in NNeo/3-5B/ΔGDD (Ikeda et al., 2002) with a cDNA cassette containing EMCV IRES, firefly luciferase gene and FMDV 2a autoprotease, with the latter directly fused to the N-terminus of NS3. In addition, the start codon of core was converted to a termination codon (TAG).

Replicon RNAs were prepared from plasmid DNA templates linearized with XbaI (pSGRmJFH1BlaRL, pSGRmJFH1BlaRL/GND and NmLuc/ΔGDD) and XmaI (pHAV-Luc) using the T7 Megascript kit (Ambion) and were purified by DNase I treatment and LiCl precipitation. RNAs were quantified by optical density, and the quality and concentration were confirmed by agarose gel electrophoresis.

Cells and transfections

Human hepatoma cells Huh7.5 and Huh7, African green monkey kidney cells FRhK4 and Vero-E6 were maintained by conventional techniques. MDBK cells were cultured in Dulbecco's modified Eagle's medium supplemented with 10% horse serum, penicillin and streptomycin. HEK293 FLP-IN T-Rex cells expressing ISG20 and mutant ISG20 were cultured as described (Jiang et al., 2008). Huh7.5 and MDBK cells stably expressing ISG20, the catalytically inactive mutant ISG20, ISG20L1, or the control vector were established by transducing cells with replication incompetent retroviruses encoding WT (pCX4Bsr-ISG20-myc), D94G mutant ISG20 (pCX4Bsr-ISG20m-myc), ISG20L1 (pCX4Bsr-ISG20L1), or the empty pCX4bsr vector, respectively, followed by selection with 5 μg/ml of blasticidin (Invivogen) for ~3 weeks, as described previously (Chen et al., 2007; Wang et al., 2009). Replicon RNAs were transfected into Huh7.5 derived cells using DMRIE-C transfection reagent (Invitrogen) at a ratio of 5 μg of lipid to 1 μg of RNA, as described (Lanford et al., 2003). DNA transfection of Huh7.5 derived cells was conducted using TransIT-LT1 (Mirus) per manufacturer's instructions. In some experiments, replicon RNAs and plasmids were cotransfected into Huh7 cells using Lipofectamine 2000 as suggested by the manufacturer (Invitrogen).

Viruses

Cell culture derived HCV (JFH1 virus) stocks were produced by transfection of Huh7.5 cells with *in vitro* transcribed JFH1 RNA and titrated by FFU assay following immunostaining of HCV core as described (Wakita et al., 2005; Yi et al., 2006). The cytopathic NADL strain of BVDV was a gift from I. Frolov. BVDV stocks were prepared in MDBK cells and titrated by TCID50 assay. The Urbani strain of SARS-CoV was provided by L.M. Haynes and T. G. Ksiazek at the Centers for Disease Control and Prevention, Atlanta, GA. SARS-CoV stocks were grown and titrated in Vero E6 cells (Devaraj et al., 2007). Wild-type YFV Asibi strain was provided by Dr. Robert Tesh (University of Texas Medical Branch (UTMB), Galveston TX and World Reference Collection for Emerging Viruses and Arboviruses [WRCEVA]). The vaccine strain, YFV 17-D-204, was derived from the 17-D infectious clone (Rice et al., 1989) and was provided by Dr. Alan Barrett (UTMB). YFV stocks were grown in VERO-E6 cells (ATCC) and harvested 4 days post-infection or when cytopathic effects were first visible. HM175/18f is a rapidly replicating, cell culture-adapted variant of HAV (Lemon et al., 1991). Working stocks were produced in Huh7 cells. Experiments involving virulent YFV and SARS-CoV were conducted in

approved biosafety level-3 laboratories at UTMB. Sendai virus stocks (Cantell strain) were purchased from Charles River Laboratories.

Virus titration assays

Infectious progeny virus yields in cell-free culture supernatants of HCV and YFV infected cultures were determined by focus forming assay and viral titers were expressed as FFU/ml. Details for HCV FFU titration assay has been presented elsewhere (Wakita et al., 2005; Yi et al., 2006). For titration of YFV yields, Vero-E6 cells were infected with the serial dilutions from time course supernatant samples for 1 h at 37 °C, 5% CO_2 with occasional rocking followed by an overlay of 1% agarose/1X MEM (Sigma) supplemented with 2% bovine growth serum (Hyclone). Plates were incubated for 4 days at 37 °C, 5% CO_2 and then fixed with 10% buffered formalin (Sigma). Cells were permeabilized with 70% ethanol, washed twice with PBS, and anti-YFV mouse hyperimmune ascitic fluid (kindly provided by Robert Tesh, WRCEVA) in PBS solution containing 5% milk and 1% Tween 20 (Sigma) were added and incubated overnight with rocking. Cells were then washed twice with PBS and incubated with goat anti-mouse IgG HRP-conjugated antibody (Dako) in solution with PBS supplemented with 1% non-sterile bovine growth serum and incubated for 5 h at room temperature. Cells were washed twice with PBS followed by staining with AEC Substrate Chromagen (Dako) focus forming unit visualization.

BVDV and SARS-CoV infectious progeny virus yields were determined by a standard $TCID_{50}$ assay based on observation of cytopathic effect on MDBK (for BVDV NADL) and Vero E6 (for SARS-CoV) cell monolayers in 96-well plates with a series of 10-fold-diluted samples, as described (Devaraj et al., 2007). The titer was expressed as $TCID_{50}$/ml. The titer of infectious HAV was determined by an infra-red fluorescence focus assay as described (Jangra et al., 2010).

HCV RNA stability assay

Five millions of 7.5-Bsr, 7.5-ISG20 and 7.5-ISG20m cells were electroporated with 5 μg of in vitro transcribed SGRmJFH1BlaRL/GND or NmLuc/ΔGDD RNAs using a BioRad GenePulser XCell system. The parameters used were 160 V, 500 μF, and maximum resistance. After electroporation, cells were cultured in 12-well plates for the indicated time periods prior to cell lysis (from duplicated wells) in 1X passive lysis buffer (Promega) and measurement of Renilla (for SGRmJFH1BlaRL/GND RNA transfected cells) or Firefly (for NmLuc/ΔGDD RNA transfected cells) luciferase activities in cell lysates. The luciferase activity at 3 h post transfection was set as 100% for calculation of percent luciferase activities at later time points, which were used to compare the rate of HCV RNA degradation.

RT-PCR

Following the indicated treatments, total cellular RNA was extracted from Huh7, 7.5-Bsr and 7.5-ISG20m cells using TRIzol reagent (Invitrogen) and treated with DNase I to remove genomic DNA contamination. The abundance of cellular mRNAs specific to human ISG56 and MxA genes was determined by quantitative real-time RT-PCR using commercially available primers and Taqman probes (Applied Biosystems). ISG20 mRNA quantification was conducted by SYBR green-based quantitative real-time RT-PCR using primers ISG20-409-F (5′-CTCCTGCACAAGAGCATCCA-3′) and ISG20-474-R (5′-CGTTGCCCTCGCATCTTC-3′).

Immunoblot analysis

Cellular extracts were prepared and subjected to immunoblot analysis as described (Li et al., 2005a,b). The following mAbs or polyclonal (pAb) antibodies were used: anti-FLAG M2 and anti-actin mAbs (Sigma); anti-myc tag mAb 9B11 (Cell Signaling Tech.); anti-ISG20 mAb (Abnova); rabbit anti-YFV NS3 pAb (from Charles Rice); rabbit anti-core pAb (from John McLauchlan); K24F2 anti-HAV mAb (Commonwealth Serum Institute), rabbit anti-ISG56 pAb (Wang et al., 2009); anti-Sendai virus pAb (from Ilkka Julkunen); rabbit anti-SARS-CoV N pAb (Imgenex); peroxidase-conjugated secondary goat anti-rabbit, and goat anti-mouse pAbs (Southern Biotech). Protein bands were visualized using enhanced chemiluminescence (Millipore), followed by exposure to X-ray films.

Acknowledgments

This work was supported in part by NIH grants R01-AI069285 (KL) and U19-AI040035 and R21-AI081058 (SML) and an American Cancer Society Institutional Research Grant 96-152-07 (KL). ZZ was supported by a Visiting Scholarship from the China Scholarship Council and a Natural Science Foundation Project of Chongqing (CSTC, 2009BB5063). We thank Takaji Wakita for JFH1 cDNAs, Charles Rice for Huh7.5 cells, YFV NS3 antiserum and pFL-J6/JFH-5′C19Rluc2AUbi cDNA, John McLauchlan for HCV core antiserum, Guangxiang Luo for pSGR-JFH1-Blast cDNA, Robert Tesh and Alan Barrett for YFVs, Thomas Ksiazek and Lia Haynes for SARS-CoV.

References

Akagi, T., Sasai, K., Hanafusa, H., 2003. Refractory nature of normal human diploid fibroblasts with respect to oncogene-mediated transformation. Proc. Natl. Acad. Sci. U. S. A. 100 (23), 13567–13572.
Bigger, C.B., Brasky, K.M., Lanford, R.E., 2001. DNA microarray analysis of chimpanzee liver during acute resolving hepatitis C virus infection. J. Virol. 75 (15), 7059–7066.
Blight, K.J., McKeating, J.A., Rice, C.M., 2002. Highly permissive cell lines for subgenomic and genomic hepatitis C virus RNA replication. J. Virol. 76 (24), 13001–13014.
Buckwold, V.E., Beer, B.E., Donis, R.O., 2003. Bovine viral diarrhea virus as a surrogate model of hepatitis C virus for the evaluation of antiviral agents. Antiviral Res. 60 (1), 1–15.
Chang, K.S., Cai, Z., Zhang, C., Sen, G.C., Williams, B.R., Luo, G., 2006. Replication of hepatitis C virus (HCV) RNA in mouse embryonic fibroblasts: protein kinase R (PKR)-dependent and PKR-independent mechanisms for controlling HCV RNA replication and mediating interferon activities. J. Virol. 80 (15), 7364–7374.
Chen, Z., Rijnbrand, R., Jangra, R.K., Devaraj, S.G., Qu, L., Ma, Y., Lemon, S.M., Li, K., 2007. Ubiquitination and proteasomal degradation of interferon regulatory factor-3 induced by Npro from a cytopathic bovine viral diarrhea virus. Virology 366 (2), 277–292.
Cinatl, J., Morgenstern, B., Bauer, G., Chandra, P., Rabenau, H., Doerr, H.W., 2003. Treatment of SARS with human interferons. Lancet 362 (9380), 293–294.
Coute, Y., Kindbeiter, K., Belin, S., Dieckmann, R., Duret, L., Bezin, L., Sanchez, J.C., Diaz, J.J., 2008. ISG20L2, a novel vertebrate nucleolar exoribonuclease involved in ribosome biogenesis. Mol. Cell. Proteomics 7 (3), 546–559.
de Lang, A., Baas, T., Teal, T., Leijten, L.M., Rain, B., Osterhaus, A.D., Haagmans, B.L., Katze, M.G., 2007. Functional genomics highlights differential induction of antiviral pathways in the lungs of SARS-CoV-infected macaques. PLoS Pathog. 3 (8), e112.
Degols, G., Eldin, P., Mechti, N., 2007. ISG20, an actor of the innate immune response. Biochimie 89 (6–7), 831–835.
Devaraj, S.G., Wang, N., Chen, Z., Tseng, M., Barretto, N., Lin, R., Peters, C.J., Tseng, C.T., Baker, S.C., Li, K., 2007. Regulation of IRF-3-dependent innate immunity by the papain-like protease domain of the severe acute respiratory syndrome coronavirus. J. Biol. Chem. 282 (44), 32208–32221.
Espert, L., Degols, G., Gongora, C., Blondel, D., Williams, B.R., Silverman, R.H., Mechti, N., 2003. ISG20, a new interferon-induced RNase specific for single-stranded RNA, defines an alternative antiviral pathway against RNA genomic viruses. J. Biol. Chem. 278 (18), 16151–16158.
Espert, L., Degols, G., Lin, Y.L., Vincent, T., Benkirane, M., Mechti, N., 2005. Interferon-induced exonuclease ISG20 exhibits an antiviral activity against human immunodeficiency virus type 1. J. Gen. Virol. 86 (Pt 8), 2221–2229.
Espert, L., Eldin, P., Gongora, C., Bayard, B., Harper, F., Chelbi-Alix, M.K., Bertrand, E., Degols, G., Mechti, N., 2006. The exonuclease ISG20 mainly localizes in the nucleolus and the Cajal (Coiled) bodies and is associated with nuclear SMN protein-containing complexes. J. Cell. Biochem. 98 (5), 1320–1333.
Flodstrom-Tullberg, M., Hultcrantz, M., Stotland, A., Maday, A., Tsai, D., Fine, C., Williams, B., Silverman, R., Sarvetnick, N., 2005. RNase L and double-stranded RNA-dependent protein kinase exert complementary roles in islet cell defense during coxsackievirus infection. J. Immunol. 174 (3), 1171–1177.
Guix, S., Asanaka, M., Katayama, K., Crawford, S.E., Neill, F.H., Atmar, R.L., Estes, M.K., 2007. Norwalk virus RNA is infectious in mammalian cells. J. Virol. 81 (22), 12238–12248.
Haagmans, B.L., Kuiken, T., Martina, B.E., Fouchier, R.A., Rimmelzwaan, G.F., van Amerongen, G., van Riel, D., de Jong, T., Itamura, S., Chan, K.H., Tashiro, M., Osterhaus, A.D., 2004. Pegylated interferon-alpha protects type 1 pneumocytes against SARS coronavirus infection in macaques. Nat. Med. 10 (3), 290–293.
Hao, Y., Yang, D., 2008. Cloning, eukaryotic expression of human ISG20 and preliminary study on the effect of its anti-HBV. J. Huazhong Univ. Sci. Technolog. Med. Sci. 28 (1), 11–13.

Hattermann, K., Muller, M.A., Nitsche, A., Wendt, S., Donoso Mantke, O., Niedrig, M., 2005. Susceptibility of different eukaryotic cell lines to SARS-coronavirus. Arch. Virol. 150 (5), 1023–1031.
Ikeda, M., Yi, M., Li, K., Lemon, S.M., 2002. Selectable subgenomic and genome-length dicistronic RNAs derived from an infectious molecular clone of the HCV-N strain of hepatitis C virus replicate efficiently in cultured Huh7 cells. J. Virol. 76 (6), 2997–3006.
Jangra, R.K., Yi, M., Lemon, S.M., 2010. DDX6 (Rck/p54) is required for efficient hepatitis C virus replication but not IRES-directed translation. J. Virol. 84 (13), 6810-6824.
Jiang, D., Guo, H., Xu, C., Chang, J., Gu, B., Wang, L., Block, T.M., Guo, J.T., 2008. Identification of three interferon-inducible cellular enzymes that inhibit the replication of hepatitis C virus. J. Virol. 82 (4), 1665–1678.
Jiang, D., Weidner, J.M., Qing, M., Pan, X.B., Guo, H., Xu, C., Zhang, X., Birk, A., Chang, J., Shi, P.Y., Block, T.M., Guo, J.T., 2010. Identification of five interferon-induced cellular proteins that inhibit west Nile virus and dengue virus infection. J. Virol. 84 (16), 8332–8341.
Kato, T., Date, T., Miyamoto, M., Furusaka, A., Tokushige, K., Mizokami, M., Wakita, T., 2003. Efficient replication of the genotype 2a hepatitis C virus subgenomic replicon. Gastroenterology 125 (6), 1808–1817.
Keskinen, P., Nyqvist, M., Sareneva, T., Pirhonen, J., Melen, K., Julkunen, I., 1999. Impaired antiviral response in human hepatoma cells. Virology 263 (2), 364–375.
Lanford, R.E., Guerra, B., Lee, H., Averett, D.R., Pfeiffer, B., Chavez, D., Notvall, L., Bigger, C., 2003. Antiviral effect and virus-host interactions in response to alpha interferon, gamma interferon, poly(i)-poly(c), tumor necrosis factor alpha, and ribavirin in hepatitis C virus subgenomic replicons. J. Virol. 77 (2), 1092–1104.
Lanford, R.E., Guerra, B., Lee, H., Chavez, D., Brasky, K.M., Bigger, C.B., 2006. Genomic response to interferon-alpha in chimpanzees: implications of rapid downregulation for hepatitis C kinetics. Hepatology 43 (5), 961–972.
Lee, J.H., Koh, Y.A., Cho, C.K., Lee, S.J., Lee, Y.S., Bae, S., 2005. Identification of a novel ionizing radiation-induced nuclease, AEN, and its functional characterization in apoptosis. Biochem. Biophys. Res. Commun. 337 (1), 39–47.
Lemon, S.M., Murphy, P.C., Shields, P.A., Ping, L.H., Feinstone, S.M., Cromeans, T., Jansen, R.W., 1991. Antigenic and genetic variation in cytopathic hepatitis A virus variants arising during persistent infection: evidence for genetic recombination. J. Virol. 65, 2056–2065.
Lerat, H., Shimizu, Y.K., Lemon, S.M., 2000. Cell type-specific enhancement of hepatitis C virus internal ribosome entry site-directed translation due to 5′ nontranslated region substitutions selected during passage of virus in lymphoblastoid cells. J. Virol. 74 (15), 7024–7031.
Li, K., Chen, Z., Kato, N., Gale Jr., M., Lemon, S.M., 2005a. Distinct poly(I-C) and virus-activated signaling pathways leading to interferon-beta production in hepatocytes. J. Biol. Chem. 280 (17), 16739–16747.
Li, K., Foy, E., Ferreon, J.C., Nakamura, M., Ferreon, A.C., Ikeda, M., Ray, S.C., Gale Jr., M., Lemon, S.M., 2005b. Immune evasion by hepatitis C virus NS3/4A protease-mediated cleavage of the Toll-like receptor 3 adaptor protein TRIF. Proc. Natl. Acad. Sci. U. S. A. 102 (8), 2992–2997.
Lohmann, V., Korner, F., Koch, J., Herian, U., Theilmann, L., Bartenschlager, R., 1999. Replication of subgenomic hepatitis C virus RNAs in a hepatoma cell line. Science 285 (5424), 110–113.
MacDonald, M.R., Machlin, E.S., Albin, O.R., Levy, D.E., 2007. The zinc finger antiviral protein acts synergistically with an interferon-induced factor for maximal activity against alphaviruses. J. Virol. 81 (24), 13509–13518.
Martin, A., Lemon, S.M., 2006. Hepatitis A virus: from discovery to vaccines. Hepatology 43 (2 Suppl 1), S164–S172.
Muller, S., Geffers, R., Gunther, S., 2007. Analysis of gene expression in Lassa virus-infected HuH-7 cells. J. Gen. Virol. 88 (Pt 5), 1568–1575.
Nguyen, L.H., Espert, L., Mechti, N., Wilson III, D.M., 2001. The human interferon- and estrogen-regulated ISG20/HEM45 gene product degrades single-stranded RNA and DNA in vitro. Biochemistry 40 (24), 7174–7179.
Peiris, J.S., Yuen, K.Y., Osterhaus, A.D., Stohr, K., 2003. The severe acute respiratory syndrome. N. Engl. J. Med. 349 (25), 2431–2441.
Peiris, J.S., Guan, Y., Yuen, K.Y., 2004. Severe acute respiratory syndrome. Nat. Med. 10 (12 Suppl), S88–S97.
Rice, C.M., Grakoui, A., Galler, R., Chambers, T.J., 1989. Transcription of infectious yellow fever RNA from full-length cDNA templates produced by in vitro ligation. New Biol. 1 (3), 285–296.
Saito, T., Owen, D.M., Jiang, F., Marcotrigiano, J., Gale Jr., M., 2008. Innate immunity induced by composition-dependent RIG-I recognition of hepatitis C virus RNA. Nature 454 (7203), 523–527.
Samuel, M.A., Whitby, K., Keller, B.C., Marri, A., Barchet, W., Williams, B.R., Silverman, R. H., Gale Jr., M., Diamond, M.S., 2006. PKR and RNase L contribute to protection against lethal West Nile Virus infection by controlling early viral spread in the periphery and replication in neurons. J. Virol. 80 (14), 7009–7019.
Sen, G.C., 2001. Viruses and interferons. Annu. Rev. Microbiol. 55, 255–281.
Silverman, R.H., 2007. Viral encounters with 2′, 5′-oligoadenylate synthetase and RNase L during the interferon antiviral response. J. Virol. 81 (23), 12720–12729.
Spiegel, M., Pichlmair, A., Muhlberger, E., Haller, O., Weber, F., 2004. The antiviral effect of interferon-beta against SARS-coronavirus is not mediated by MxA protein. J. Clin. Virol. 30 (3), 211–213.
Stark, G.R., Kerr, I.M., Williams, B.R., Silverman, R.H., Schreiber, R.D., 1998. How cells respond to interferons. Annu. Rev. Biochem. 67, 227–264.
Sumpter Jr., R., Loo, Y.M., Foy, E., Li, K., Yoneyama, M., Fujita, T., Lemon, S.M., Gale Jr., M., 2005. Regulating intracellular antiviral defense and permissiveness to hepatitis C virus RNA replication through a cellular RNA helicase, RIG-I. J. Virol. 79 (5), 2689–2699.
Tang, B.S., Chan, K.H., Cheng, V.C., Woo, P.C., Lau, S.K., Lam, C.C., Chan, T.L., Wu, A.K., Hung, I.F., Leung, S.Y., Yuen, K.Y., 2005. Comparative host gene transcription by microarray analysis early after infection of the Huh7 cell line by severe acute respiratory syndrome coronavirus and human coronavirus 229E. J. Virol. 79 (10), 6180–6193.
Tscherne, D.M., Jones, C.T., Evans, M.J., Lindenbach, B.D., McKeating, J.A., Rice, C.M., 2006. Time- and temperature-dependent activation of hepatitis C virus for low-pH-triggered entry. J. Virol. 80 (4), 1734–1741.
Wakita, T., Pietschmann, T., Kato, T., Date, T., Miyamoto, M., Zhao, Z., Murthy, K., Habermann, A., Krausslich, H.G., Mizokami, M., Bartenschlager, R., Liang, T.J., 2005. Production of infectious hepatitis C virus in tissue culture from a cloned viral genome. Nat. Med. 11 (7), 791–796.
Wang, N., Liang, Y., Devaraj, S., Wang, J., Lemon, S.M., Li, K., 2009. Toll-like receptor 3 mediates establishment of an antiviral state against hepatitis C virus in hepatoma cells. J. Virol. 83 (19), 9824–9834.
Wieland, S., Thimme, R., Purcell, R.H., Chisari, F.V., 2004. Genomic analysis of the host response to hepatitis B virus infection. Proc. Natl. Acad. Sci. U. S. A. 101 (17), 6669–6674.
Yi, M., Lemon, S.M., 2002. Replication of subgenomic hepatitis A virus RNAs expressing firefly luciferase is enhanced by mutations associated with adaptation of virus to growth in cultured cells. J. Virol. 76 (3), 1171–1180.
Yi, M., Villanueva, R.A., Thomas, D.L., Wakita, T., Lemon, S.M., 2006. Production of infectious genotype 1a hepatitis C virus (Hutchinson strain) in cultured human hepatoma cells. Proc. Natl. Acad. Sci. U. S. A. 103 (7), 2310–2315.
Yoneyama, M., Fujita, T., 2010. Recognition of viral nucleic acids in innate immunity. Rev. Med. Virol. 20 (1), 4–22.
Zhang, Y., Burke, C.W., Ryman, K.D., Klimstra, W.B., 2007. Identification and characterization of interferon-induced proteins that inhibit alphavirus replication. J. Virol. 81 (20), 11246–11255.
Zheng, X., Silverman, R.H., Zhou, A., Goto, T., Kwon, B.S., Kaufman, H.E., Hill, J.M., 2001. Increased severity of HSV-1 keratitis and mortality in mice lacking the 2-5A-dependent RNase L gene. Invest. Ophthalmol. Vis. Sci. 42 (1), 120–126.
Zheng, B., He, M.L., Wong, K.L., Lum, C.T., Poon, L.L., Peng, Y., Guan, Y., Lin, M.C., Kung, H.F., 2004. Potent inhibition of SARS-associated coronavirus (SCOV) infection and replication by type I interferons (IFN-alpha/beta) but not by type II interferon (IFN-gamma). J. Interferon Cytokine Res. 24 (7), 388–390.
Zhou, A., Paranjape, J., Brown, T.L., Nie, H., Naik, S., Dong, B., Chang, A., Trapp, B., Fairchild, R., Colmenares, C., Silverman, R.H., 1997. Interferon action and apoptosis are defective in mice devoid of 2′, 5′-oligoadenylate-dependent RNase L. EMBO J. 16 (21), 6355–6363.
Zhou, A., Paranjape, J.M., Der, S.D., Williams, B.R., Silverman, R.H., 1999. Interferon action in triply deficient mice reveals the existence of alternative antiviral pathways. Virology 258 (2), 435–440.